MASS TRANSFER FROM A PACKED BED TO A WELL STIRRED SOLUTION AND THE MEASUREMENT OF THE EFFECTIVE PSEUDO-DIFFUSIVITY OF COD IN FEEDLOT RUNOFF THROUGH A POROUS STRATUM

by 45

SO KWANG CHOI

B. S., Seoul National University, 1966

A MASTER'S THESIS

submitted in partial fulfillment of the

requirements for the degree

MASTER OF SCIENCE

Department of Chemical Engineering

KANSAS STATE UNIVERSITY
Manhattan, Kansas

1969

Approved by:

L. T. Fan

Major Professor

LD
2668
T4
1969
C45

TABLE OF CONTENTS

Chapter		Page
I	INTRODUCTION	1
II	DERIVATION OF THE MATHEMATICAL MODEL OF THE SYSTEM	6
III	ANALYTICAL SOLUTIONS OF THE SYSTEM EQUATIONS	12
IV	EXPERIMENT WITH AQUEOUS SUCROSE SOLUTION	46
V	TRANSPORT RATE OF COD BY DIFFUSION THROUGH A PORous PACKED BED SATURATED BY WATER	68
NOMENCLATURE		85
ACKNOWLEDGMENTS		88
BIBLIOGRAPHY		89
APPENDICES		91

CHAPTER I

INTRODUCTION

Modern industrial and agricultural products have been accompanied by many new waste by-products, which it is hoped, are reasonably utilized and should, at least, be sanitarily disposed of.

This investigation is concerned with water pollution which is caused by farm wastes — especially, farm animal waste. As Henderson (1) and Smith and Miner (2) pointed out, the stream pollution by rural land drainage from a watershed with farm animals, especially commercial cattle can be significant in terms of total demand on stream oxygen resources.

According to Miner and four members of ASAE (3), the quality parameters in cattle feedlot runoff are

(1) organic matter
(2) nitrogen compounds
(3) suspended solids
(4) bacterial populations and
(5) other chemicals.

These waste substances may be classified in three groups: organics, organisms and inorganics.

Smith and Miner (2) pointed out that runoff from a cattle feedlot pollutes the water by causing a lack of dissolved oxygen and/or high ammonia-nitrogen concentrations. When the oxygen content of the water becomes sufficiently decreased, fish, other aquatic animals, and plant life are killed. So, consideration has

to be given to the lack of dissolved oxygen in a waste water. Chemical oxygen demand (COD) which represents the chemical oxygen required to oxidize the organic material can be used as a quantitative measure for the organic matter in the waste water.

As mentioned by Sawyer (5), the COD test can be used as a means of measuring the pollutional strength of waste water because it is based upon the fact that all organic compounds, with a few exceptions, can be oxidized to carbon dioxide and water by the action of strong oxidizing agents under acid conditions, Generally, during the determination of COD, organic matter is converted to carbon dioxide and water regardless of the biological assimilability of the substances. As a result, COD values are greater than biochemical oxygen demand (BOD) values and may be much greater when significant amounts of biologically resistant organic matter are present. Cattle manure has a high content of lignin which is a biologically resistant organic. That is, as stated in Miner's thesis (4), COD is much greater than BOD in the analytical results of both cattle feedlot runoff and cattle manure. Besides, the COD test has the important advantage in the short time required for evaluation. This determination can be made in about three hours while a BOD test requires more than five days. Hence, COD is usually chosen rather than BOD as the index of the pollutional strength of the waste water. Here, COD is assumed to represent a hypothetical compound, so that COD concentration means the concentration of organic matter measured by its COD test.

The primary purpose of this research is to investigate the rate of transport, specifically that by molecular diffusion, of COD through a porous stratum saturated by water such as the soil-manure surface in a feedlot. If the concentration of COD in the water phase of the porous stratum is larger than that in the water on the surface of the feedlot, COD will be transported to the surface waters by molecular diffusion. In order to predict the transfer rate of COD by diffusion, the diffusion coefficient of COD in water is needed. The secondary purpose of this research is to determine this diffusion coefficient experimentally.

In this study the artificial packed bed system shown in Figure 1 was employed to simulate the soil-manure system saturated by water. The system consisted of two parts, the packed bed saturated with solute-concentrated solution, and the well stirred solute-dilute solution. When the two solutions are brought into contact, solute is transfered from the packed bed to the well stirred solution because of the concentration difference. For this system, the analytical expressions were derived as a function of time for the upper well stirred solution and as function of time and position for the lower packed bed.

Before this system was used to measure the diffusion rate of COD, it was tested by using a sucrose solution whose diffusivity was known. The transient diffusion with biochemical reaction in both parts of the system shown in Figure 1 was also considered mathematically.

It is obvious that without a system of reducing organic matter to a form in which its elements may be used again, almost

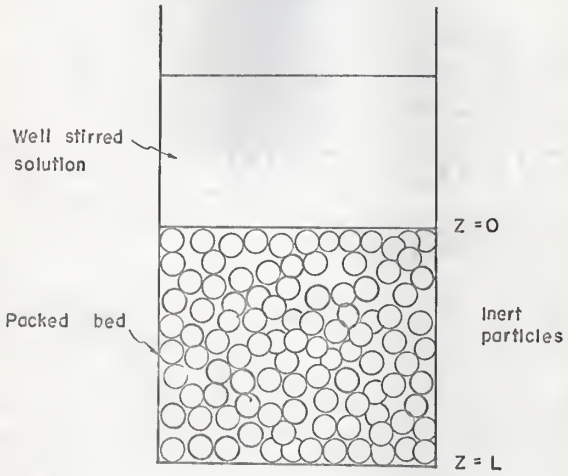

Fig. I Packed bed for simulation of a stratum (sideview).

all life would shortly cease on this earth. Micro-organisms with systems of extracellular and intracellular catalysts or enzymes function in the scheme of life to reduce these materials, secure energy from them and build new protoplasm. The biological reduction of these organic materials(waste) is dependent upon the synthesis of new bacterial protoplasm from them (6).

Usually, there are a number of diverse free-living forms of Micro-organisms in animal waste. Each of these reduces a different kind of organic material in its proper environment. This overall reduction can be considered as an approximate first order irreversible chemical reaction.

For this case, the analytical expressions were derived as a function of time for the upper well stirred solution and as a function of time and position for the lower packed bed. When the value of diffusivity is known, the chemical reaction constant can be determined by forcing the experimental data to fit the mathematical expression.

CHAPTER II

DERIVATION OF THE MATHEMATICAL MODEL OF THE SYSTEM

In this chapter, the system equations which characterize the diffusion process taking place in the system and the corresponding initial and boundary conditions will be derived. For this purpose, the system under consideration (Figure 1) is assumed to contain a binary liquid mixture. Actually, a solution of manure in water is a very complex liquid mixture.

The packed bed has a porosity F, cross-sectional area A, and tortuosity T. The packed bed is assumed to be saturated with a binary solution and to have a uniform initial concentration c_i, based on the void space. The solution in the upper reservoir has a volume V and initial concentration c_{1i}.

If the density of this binary solution increases with its concentration, the initial concentration of the solution within the packed bed should be higher than that of the upper reservoir solution, so that no bulk flow will occur.

Mass transfer occurs because of the concentration difference between the upper solution and the solution within the packed bed. If there is no bulk flow, mass transfer is due to only molecular diffusion.

The following assumptions are made:

(1) The porous packed bed is a homogeneous solution layer.

(2) Solid particles are inert so that there is no mass transfer between the particles and the solution.

(3) The upper solution is a completely mixed solution such

that the concentration is always uniform in the reservoir.

(4) The diffusion coefficient is constant.

The problem can be considered as a one-dimensional diffusion problem with or without chemical reaction for one component. Also, two different systems are considered here, the one with finite thickness of the bed and the other with infinite thickness of the bed. All together four different cases are considered. These are

CASE (I) : Diffusion with finite thickness of the packed bed and without reaction

CASE (II) : Diffusion with finite thickness of the packed bed and with an irreversible first order homogeneous reaction

CASE (III): Diffusion with infinite thickness of the packed bed and without reaction

CASE (IV) : Diffusion with infinite thickness of the packed bed and with an irreversible first order homogeneous reaction.

Diffusion equations and initial and boundary conditions will be derived for these four cases.

CASE (I) : Diffusion with finite thickness of the packed bed and without reaction

This system is assumed to have thickness L. The diffusion of a substance through an elemental volume arbitrarily located within the packed bed is considered. By making a shell balance as

shown in Eqn. (13), the following partial differential equation, called Fick's second law of diffusion, can be obtained [see Appendix A]:

$$\frac{\partial c}{\partial t} = D_e \frac{\partial^2 c}{\partial z^2} \qquad (1).$$

The effective diffusion coefficient, D_e, in equation (1) can be related with the molecular diffusivity, D_o, as follows [see Appendix A]:

$$D_e = \frac{D_o}{T} \qquad (2).$$

If a material balance is made at the interface of two layers, the following equation can be obtained [see Appendix A]:

$$V \frac{dc_1}{dt} = D_e \left.\frac{\partial c}{\partial z}\right|_{z=0} PA \qquad \text{for } t > 0 \qquad (3).$$

For this system the following initial and boundary conditions can be established:

(1) The concentrations within the packed bed and in the upper reservoir are initially c_i and c_{1i} respectively, that is, when $t = 0$,

$$c = c_i$$

and

$$c_1 = c_{1i}.$$

(2) At the interface between two layers, the concentrations of both layers are the same, that is, at $z = 0$,

$$c = c_1 \qquad \text{for } t > 0.$$

(3) There is no mass transfer at the bottom of the bed, that

(3), at $z = L$,

$$\frac{\partial c}{\partial z} = 0.$$

Here, equations (1) and (3) are to be solved for c and c_1 with the three initial and boundary conditions described above. The analytical solutions are given in terms of dimensionless concentrations X and Y in Chapter III.

CASE (II) : Diffusion with finite thickness of the packed bed and with an irreversible first order homogeneous reaction

This case can be treated in the same manner as Case (I) with the addition of the reaction both in the completely mixed solution and within the packed bed layer. If an irreversible first order homogeneous reaction is assumed to occur, equations (1) and (3) become

$$\frac{\partial c}{\partial t} = D_e \frac{\partial^2 c}{\partial z^2} - kc \tag{4}$$

and

$$V \frac{dc_1}{dt} = D_e \left.\frac{\partial c}{\partial z}\right|_{z=0} PA - Vkc_1 \quad \text{for } t > 0 \tag{5}.$$

Initial and boundary conditions are

(1) when $t = 0$,

$$c = c_i$$

and

$$c_1 = c_{1i},$$

(2) at $z = 0$,

$$c = c_1 \quad \text{for } t > 0,$$

and

(3) at $z = L$,

$$\frac{\partial c}{\partial z} = 0$$

The analytical solutions for this problem are given in Chapter III.

CASE (III) : Diffusion with infinite thickness of the packed bed and without reaction

This case is identical to Case (I) except for one boundary condition. Therefore, for this system the following partial differential equations can be written,

$$\frac{\partial c}{\partial t} = D_e \frac{\partial^2 c}{\partial z^2} \tag{6}$$

and

$$V \frac{dc_1}{dt} = D_e \frac{\partial c}{\partial z}\bigg|_{z=0} PA \quad \text{for } t > 0 \tag{7}.$$

Since the thickness of the packed bed is assumed infinite, the initial and boundary conditions become

(1) when $t = 0$,

$$c = c_i$$

and

$$c_1 = c_{1i},$$

(2) at $z = 0$,

$$c = c_1 \quad \text{for } t > 0,$$

and

(3) at $z = \infty$,

$$c = c_i.$$

The analytical solutions for c and c_1 are also given in Chapter III.

CASE (IV) : Diffusion with infinite thickness of the packed bed and with an irreversible first order homogeneous reaction

If an irreversible first order homogeneous reaction is assumed for the solutions both in the well stirred reservoir and within the packed bed, equations (6) and (7) in Case (III) become

$$\frac{\partial c}{\partial t} = D_e \frac{\partial^2 c}{\partial z^2} - kc \tag{8}$$

and

$$V \frac{dc_1}{dt} = D_e \frac{\partial c}{\partial z}\bigg|_{z=0} FA - Vkc_1 \quad \text{for } t > 0 \tag{9}.$$

Initial and boundary conditions for this case are,

(1) when $t = 0$,

$$c = c_1$$

and

$$c_1 = c_{1i},$$

(2) at $z = 0$,

$$c = c_1 \quad \text{for } t > 0,$$

and

(3) at $z = \infty$,

$$c = c_i \exp(-kt)$$

or

$$\frac{dc}{dt} = - kc.$$

The analytical solutions are contained in Chapter III.

CHAPTER III

ANALYTICAL SOLUTIONS OF THE SYSTEM EQUATIONS

In the preceding chapter, the differential diffusion equations and initial and boundary conditions have been derived for four different cases. In this chapter, the analytical expressions will be derived for these cases.

For simplicity, two sets of dimensionless quantities are introduced. The first set is

$$\left.\begin{aligned} X &= \frac{c - c_{1i}}{c_1 - c_{1i}} \\ Y &= \frac{c_1 - c_{1i}}{c_1 - c_{1i}} \\ \theta &= \frac{D_o t}{L^2} \\ \lambda &= \frac{z}{L} \\ \alpha &= \frac{ALP}{V} \end{aligned}\right\} \qquad (10).$$

The second set is

$$\left.\begin{aligned} X &= \frac{c - c_{1i}}{c_1 - c_{1i}} \\ Y &= \frac{c_1 - c_{1i}}{c_1 - c_{1i}} \\ \theta_1 &= \frac{D_o A^3 n^3}{V^2} t \\ \lambda_1 &= \frac{Anz}{V} \end{aligned}\right\} \qquad (10.a).$$

To obtain the rate of mass transfer quantities are compared to each other, the first set is simpler and more suitable than the second for Cases (I) and (II). However, for Cases (III) and (IV), the first set, equation (10), can not be applied, but the second, equation (10.a), can be used. Equation (10.a) can also be applied to Cases (I) and (II) if desired. In the following developments, equation (10) is used for Cases (I) and (II), and equation (10.a) is used for Cases (III) and (IV). In Appendix (F), equation(10.a) is used to obtain the analytical solution for Case (II).

CASE (I) : Diffusion with finite thickness of the packed bed and without reaction

Diffusion equations, equations (1) and (3) in the preceding chapter, are repeated below;

$$\frac{\partial c}{\partial t} = D_e \frac{\partial^2 c}{\partial z^2} \tag{1}$$

and

$$V \frac{dc_1}{dt} = D_e \frac{\partial c}{\partial z}\Big|_{z=0} FA \quad \text{for } t > 0 \tag{3}.$$

The initial and boundary conditions are

(1) when $t = 0$,

$$c = c_i$$

and

$$c_1 = c_{1i},$$

(2) at $z = 0$,

$$c = c_1 \quad \text{for } t > 0,$$

(3) at $z = L$,

$$\frac{\partial c}{\partial z} = 0.$$

By substituting equation (10) into equations (1) and (3), they become

$$\frac{\partial Y}{\partial \theta} = \frac{\partial^2 Y}{\partial \lambda^2} \tag{11},$$

and

$$\frac{dY}{d\theta} = \alpha \frac{\partial Y}{\partial \lambda}\bigg|_{\lambda=0} \quad \text{for } \theta > 0 \tag{12}.$$

Accordingly, the initial and boundary conditions become

(1) when $\theta = 0$,

$$X = 1$$

and

$$Y = 0,$$

(2) at $\lambda = 0$,

$$X = Y \quad \text{for } \theta > 0,$$

and

(3) at $\lambda = 1$,

$$\frac{\partial Y}{\partial \lambda} = 0.$$

The analytical solution for this problem is available in Crank (7). In his problem, the solute is diffused from the well stirred solution to a solid plane sheet with the corresponding initial and boundary conditions. However, the final solutions listed in the book are the same as those obtained here (Case I).

This is because the zero differential equations are to be solved with corresponding initial and boundary conditions except that the diffusion proceeds in an inverse direction. That is, by using the Laplace transformation technique, the analytical solutions which give both the concentration of the solution in the upper reservoir as a function of time and the concentration of the solution within the packed bed as a function of time and distance from the interface are obtained as follows:

$$Y(\theta) = \frac{\alpha}{1+\alpha} - \sum_{n=1}^{\infty} \frac{2}{(1+\alpha+\frac{\beta_n^2}{\alpha})} \exp(-\beta_n^2\theta) \qquad (13)$$

and

$$X(\theta,\lambda) = \frac{\alpha}{1+\alpha} - \sum_{n=1}^{\infty} \frac{2\cos(\beta_n(1-\lambda))}{(1+\alpha+\frac{\beta_n^2}{\alpha})\cos\beta_n} \exp(-\beta_n^2\theta) \qquad (14),$$

where β_n satisfies the equation

$$\beta \cot\beta + \alpha = 0 \qquad (15).$$

In equation (14), it is shown that at $\lambda = 0$, $X(\theta,\lambda) = Y(\theta)$, which satisfies boundary condition (2). Also, if X and Y are plotted against θ for a given α, for example, $\alpha = 1.77276$, Figure 2 is obtained. The corresponding values of β are listed in Table 1. According to Figure 2, the concentration of the packed bed at different distances from the interface changes with respect to time, with different transient phenomena. That is, at a point near the interface, the concentration decreases quickly with respect to time and then increases to approach the final steady state value, while at a point near the bottom of the packed bed,

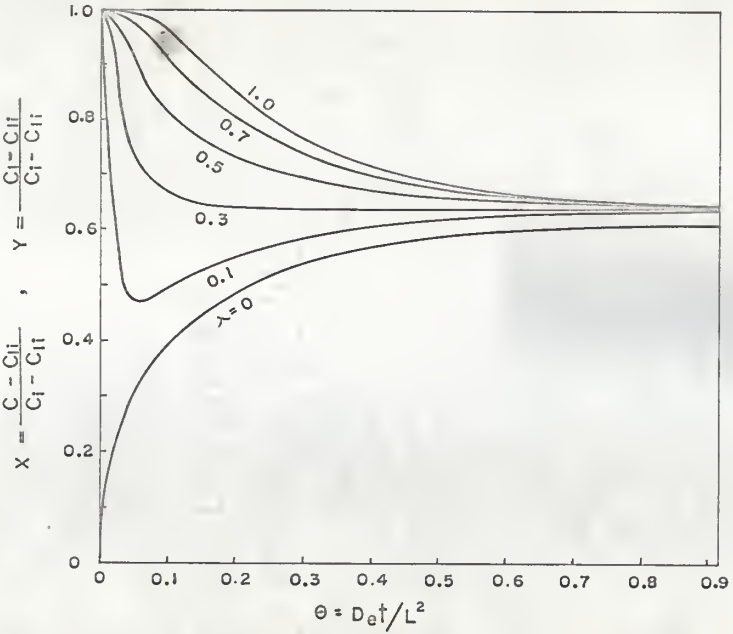

Fig. 2. Transient behavior of the concentrations X & Y (identical with X at $\lambda = 0$) when $\alpha = 1.77276$.

Table. 1. Eigenvalues which satisfy $\beta \cot\beta + \alpha = 0$ for different values of α.

eigen-values	α				
	0.59092	0.88638	1.06366	1.77276	2.48187
β_1	1.87564	1.93968	2.05193	2.24073	2.37771
β_2	4.83398	4.89157	4.16028	5.05040	5.16055
β_3	7.92830	7.96482	7.98649	8.07042	8.14914
β_4	11.04910	11.07557	11.09099	11.15325	11.21346
β_5	14.17877	14.19943	14.21194	14.26070	14.30881
β_6	17.31295	17.32997	17.34015	17.38028	17.42030
β_7	20.44926	20.46372	20.47215	20.50647	20.54050
β_8	23.58697	23.59949	23.60706	23.63672	23.66639
β_9	26.72567	26.73672	26.73842	26.76959	26.79593
β_{10}	29.86493	29.87482	29.88064	29.90449	29.92790
β_{11}	33.00460	33.01346	33.01848	33.03819	33.06175
β_{12}	36.14465	36.15272	36.15767	36.17716	36.21410
β_{13}	39.28490	39.29258	39.29684	39.31509	39.33301
β_{14}	42.42540	42.43242	42.43649	42.44639	42.46996
β_{15}.	45.56608	45.57256	45.57634	45.59205	45.60746

The concentration decreases slowly with respect to time to approach the final value. Figure 3 shows the distributions of dimensionless concentrations through the packed bed at various values of the dimensionless time θ, when α = 1.77276. From Figure 3, it is seen that the initial concentrations within the packed bed and in the well stirred reservoir are unity and zero respectively. As time goes on, the two concentrations reach a common final value.

If equations (13) and (14) are rewritten so that dimensionless concentrations may be expressed as functions of dimensional time and length,

$$Y(t) = \frac{1}{1+\frac{V}{ALF}} - \sum_{n=1}^{\infty} \frac{2 \exp(-\frac{\beta_n^2 D_e t}{L^2})}{(1+\frac{ALF}{V}+\frac{V\beta_n^2}{ALF})} \tag{16}$$

and

$$X(t,z) = \frac{1}{1+\frac{V}{ALF}} - \sum_{n=1}^{\infty} \frac{2 \cos(\beta_n(1-\frac{z}{L})) \exp(-\frac{\beta_n^2 D_e t}{L^2})}{(1+\frac{ALF}{V}+\frac{V\beta_n^2}{ALF}) \cos\beta_n} \tag{17}$$

are obtained.

If dimensionless concentrations Y and X are plotted with respect to dimensional time, t, for different values of effective diffusivity, D_e, Figures 4 and 5 are obtained for specified values of A, L, F and V corresponding to α = 1.77276. Eigenvalues from equation (15) for these values are listed in Table 1. It can be seen from Figures 4 and 5 that for large values of effective diffusivity, mass transfer occurs rapidly and the system reaches

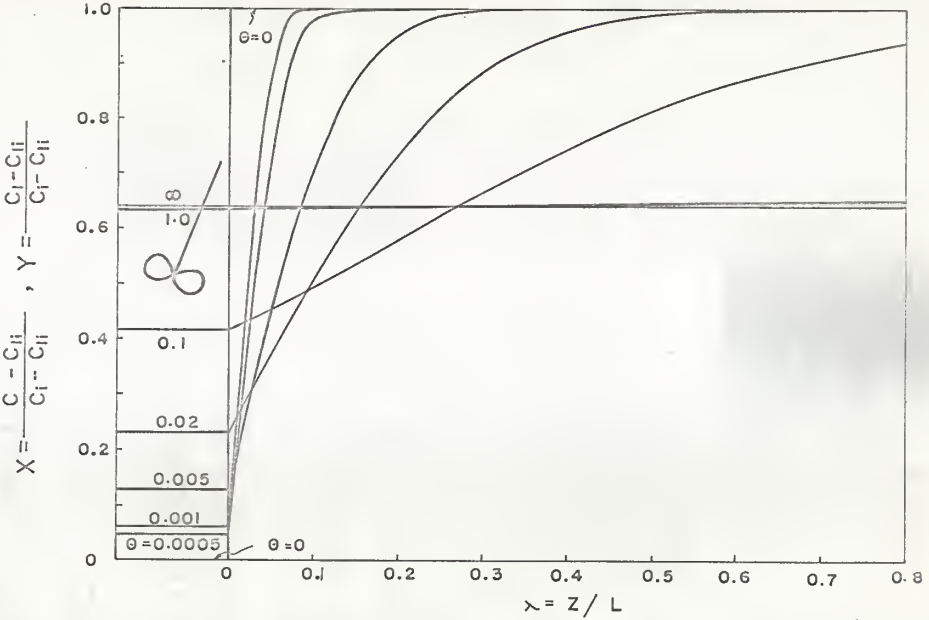

Fig. 3. Concentration profiles through the finite packed bed when $\alpha = 1.77276$.

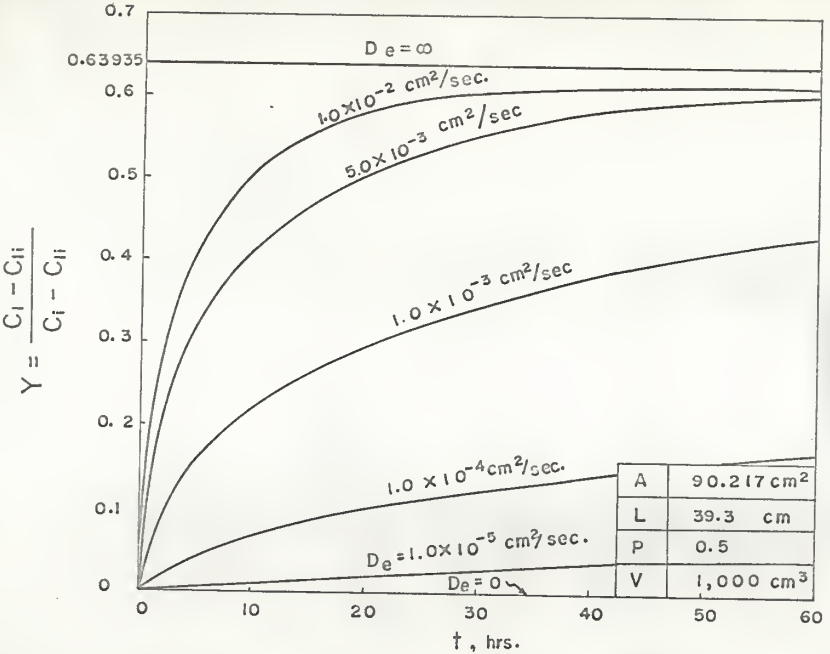

Fig. 4. Effect of the diffusivity on the concentration of the upper solution for specified values of A , L , P & V .

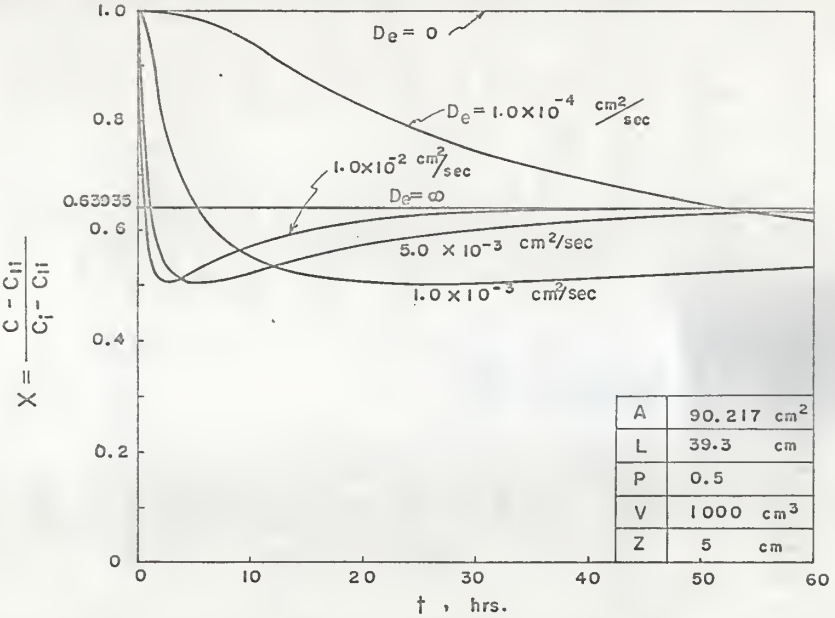

Fig. 5. Effect of the diffusivity on the concentration within the packed bed for the specified values of A, L, P, V, & Z .

the final value in a short time. If the effective diffusivity of a substance has infinite value, the concentrations in both layers reach a uniform and identical final value, a/(1+ε), immediately after the diffusion process starts. For example, for the system with infinite thickness of the packed bed, both parts of the system have unit value of concentration as soon as the layers contact. On the other hand, if the effective diffusivity of the substance is zero, no change takes place between the two layers and both concentrations remain at their initial values.

In Figures 6, 7 and 8, Y and X are expressed with respect to time, t, for different values of porosity P, packed bed length L, and upper reservoir volume V. In each figure, one of the parameters is varied while each of the others are held constant.

According to Figure 6, the concentration in the well stirred reservoir is higher for the system having a large value of porosity, than for the system having a small value of porosity. Also, at a fixed position within the packed bed, the concentration for the former system is higher than that for the latter.

Figure 7 shows that the system having a greater thickness of the packed bed has a higher final value than the system with a smaller thickness. Thus, the system having infinite thickness has the largest final value, unity.

The effect of the well stirred reservior volume on the concentrations in the upper reservior and within the packed bed is shown in Figure 8. For the case in which the upper reservior has an infinite volume of solution, Y remains zero and X approaches zero as time passes.

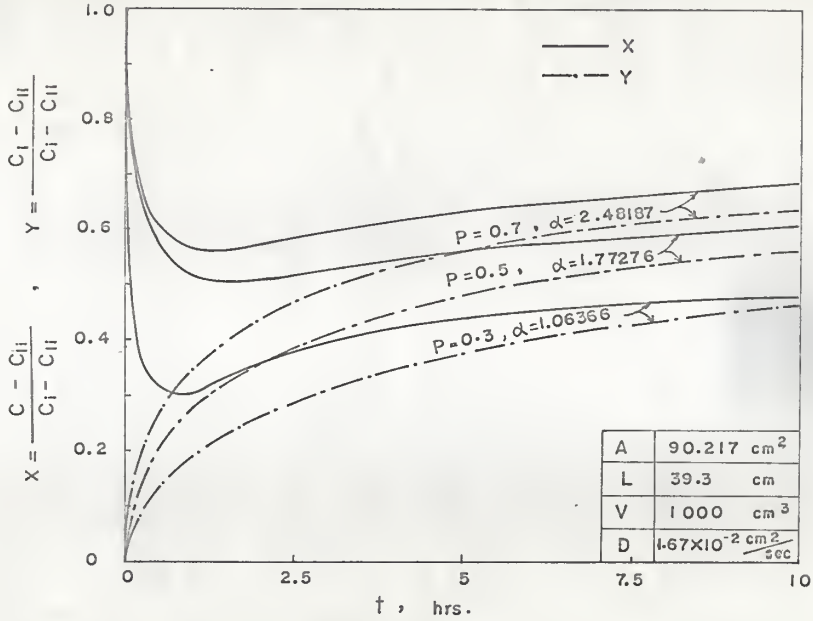

Fig. 6. Effect of the porosity on the concentrations X (at Z = 5 cm) & Y.

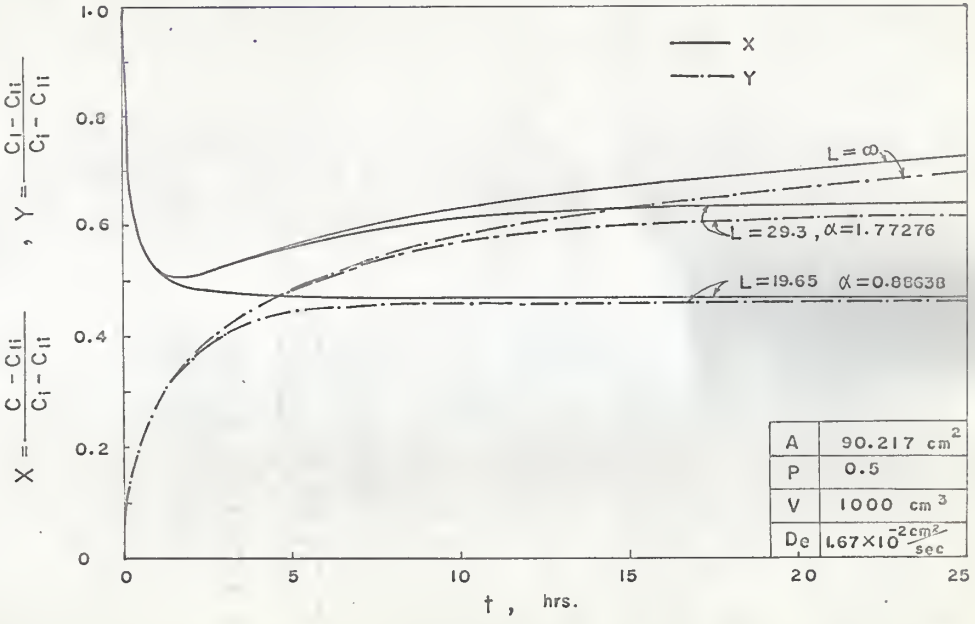

Fig. 7 Effect of the packed bed thickness on the concentrations X (at Z = 5 cm.) & Y.

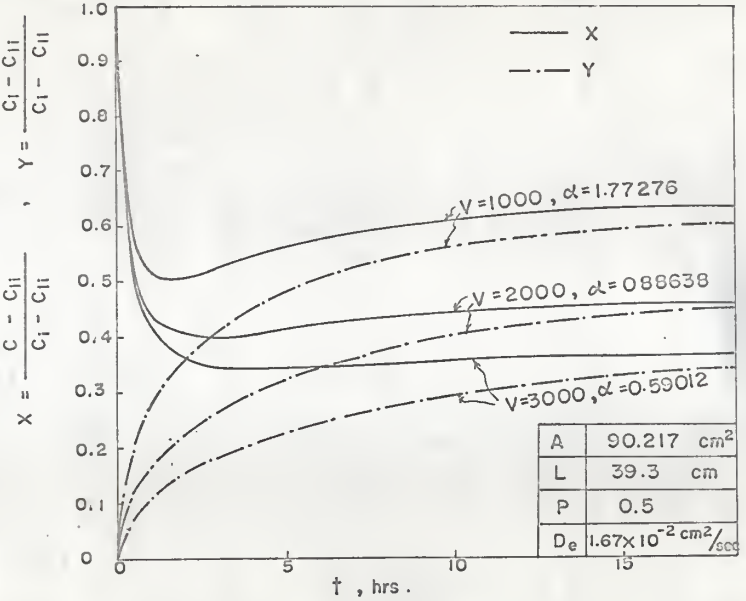

Fig. 8. Effect of the upper reservoir's volume on the concentrations X (at Z = 5 cm) & Y.

[illegible], as shown in Figure 3, if the concentration profile within the packed bed is expressed with respect to the distance from the interface at a certain moment while diffusion is proceeding, it can be seen that $\frac{\partial Y}{\partial Z} = 0$, corresponding to $\frac{\partial c}{\partial z} = 0$ at $z = L$, which satisfies boundary condition (3).

So far, many equations and figures have been illustrated. However, it can be concluded that equation (16) and Figure 4 are the most useful for the purpose of determining the diffusivity of a substance.

For all cases described above, eigenvalues are listed in Table 1.

CASE (II) : Diffusion with finite thickness of the packed bed and with an irreversible first order homogeneous reaction

The partial differential diffusion equations for this case, equations (4) and (5), are repeated below;

$$\frac{\partial c}{\partial t} = D_c \frac{\partial^2 c}{\partial z^2} - kc \qquad (4),$$

$$V \frac{dc_1}{dt} = D_c \frac{\partial c}{\partial z}\bigg|_{z=0} FA - Vkc_1 \quad \text{for } t > 0 \qquad (5).$$

Initial and boundary conditions are

(1) when $t = 0$,

$$c = c_i$$

and

$$c_1 = c_{1i},$$

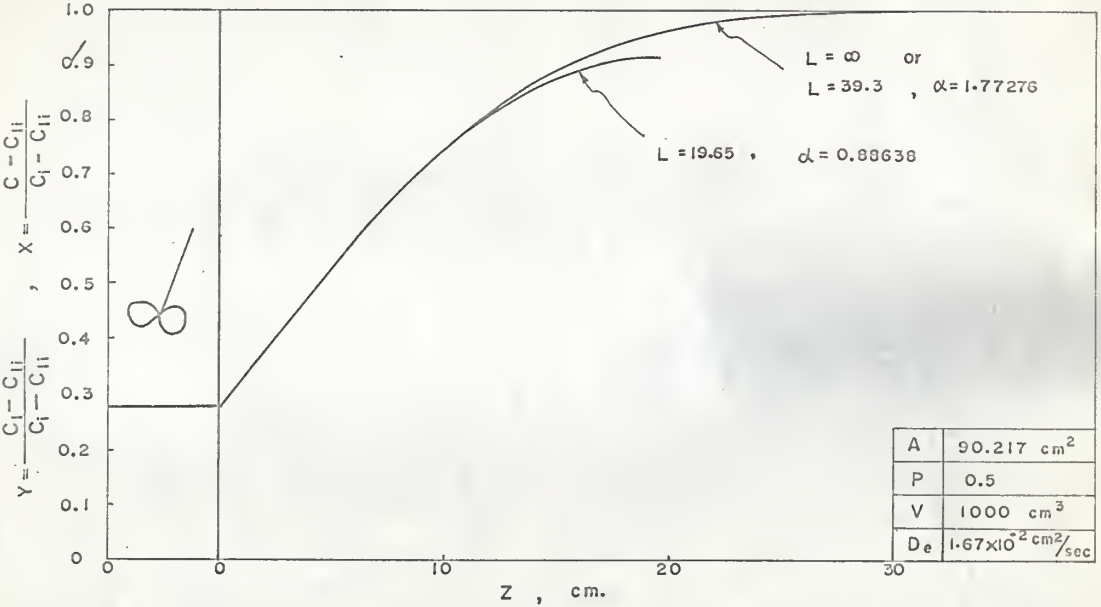

Fig. 9. Effect of the packed bed thickness on the concentration within the packed-bed at a specified time (t = 50 min.).

(2) at $z = 0$,

$$c = c_1 \quad \text{for } t > 0,$$

and

(3) at $z = L$,

$$\frac{\partial c}{\partial z} = 0.$$

By introducing equation (10) into equations (4) and (5), along with the initial and boundary conditions, the following equations can be obtained:

$$\frac{\partial Y}{\partial \theta} = \frac{\partial^2 Y}{\partial \lambda^2} - R(Y + S) \tag{18},$$

$$\frac{dY}{d\theta} + R(Y + S) = \alpha \left.\frac{\partial Y}{\partial \lambda}\right|_{\lambda=0}, \quad \text{for } \theta > 0 \tag{19}$$

with new initial and boundary conditions,

(1) when $\theta = 0$,

$$Y = 1$$

and

$$Y = 0$$

(2) at $\lambda = 0$,

$$Y = Y \quad \text{for } \theta > 0,$$

and

(3) at $\lambda = 1$,

$$\frac{\partial Y}{\partial \lambda} = 0,$$

where $R = \frac{L^2 k}{D_e}$

$$\beta = \frac{c_{21}}{(c_1 - c_{11})}.$$

This is a kind of problem in which a solute can diffuse through a porous body saturated by a solution, while simultaneously reacting chemically or biochemically, both within the porous body and the well stirred solution. Crank (9), Danckwerts (10), and Wilson (11) have described several similar problems such as problems involving diffusion in which the diffusing substance becomes immobilized within the packed bed as diffusion proceeds, a chemical reaction in which the rate of reaction depends on the rate of supply of one of the reactants by diffusion, and others. To solve these types of problems, they used the proper coordinates (cartesian, cylindrical or spherical) that were convenient for their systems. However, each of them has considered that the reaction takes place in only one part of the system, for example, only within the packed bed. This is not always the case. When microorganisms consume organic compounds in feedlot runoff, it is reasonable to consider that the utilization of organic matter takes place both in the upper well stirred solution layer and within the packed bed layer.

Now equations (18) and (19) are solved subject to the given three initial and boundary conditions. To accomplish this, Laplace transforms of equations (18) and (19) are obtained as

$$\frac{d^2\bar{x}}{d\lambda^2} - (s + R)\bar{X} + 1 - \frac{R\beta}{s} = 0 \qquad (20)$$

and

$$(s + R)\bar{Y} + \frac{\partial \bar{Y}}{\partial \lambda} = \alpha \left.\frac{\partial \bar{X}}{\partial \lambda}\right|_{\lambda=0} \qquad (21)$$

respectively. Also, transformed initial and boundary conditions are

(i) at $\lambda = 0$,

$$\bar{X} = \bar{Y} \quad \text{for } \theta > 0$$

and

(ii) at $\lambda = 1$,

$$\frac{\partial \bar{X}}{\partial \lambda} = 0.$$

Once $\bar{X}$ from equation (20) has been obtained as a function of s and λ, $\bar{Y}$ can be obtained as a function of s as shown below [see Appendix B]:

$$\bar{X} = \left[\frac{\bar{Y} - \frac{s - RS}{s(s + R)}}{1 + \exp(2\sqrt{s+R})}\right]\left[\exp((2 - \lambda)\sqrt{s+R}) + \exp(\lambda\sqrt{s+R})\right] + \frac{s - RS}{s(s + R)} \qquad (22)$$

$$\bar{Y} = \frac{\alpha\,(\exp(2\sqrt{s+R}) - 1)}{(s + R)\left[\sqrt{s+R}(\exp(2\sqrt{s+R}) + 1) + \alpha\,(\exp(2\sqrt{s+R}) - 1)\right]} + \frac{RS}{s(s + R)} \qquad (23).$$

Since,

$$\exp(2\sqrt{s+R}) - 1 = 2\exp(\sqrt{s+R})\sinh(\sqrt{s+R}) \qquad (24)$$

and

$$\exp(2\sqrt{s+R}) + 1 = 2\exp(\sqrt{s+R})\cosh(\sqrt{s+R}) \qquad (25),$$

Equation (23) becomes

$$\bar{Y} = \frac{\alpha \sinh(\lambda\sqrt{s+R})}{(s+R)[\sqrt{s+R}\cosh(\sqrt{s+R}) + \alpha \sinh(\sqrt{s+R})]} - \frac{RS}{s(s+R)} \quad (26)$$

If equations (24), (25) and (26) are substituted into equation (22), then equation (27) is obtained.

$$\bar{Y} = \frac{1}{s+R} - \frac{\sqrt{s+R}\cosh(\sqrt{s+R}(1-\lambda))}{(s+R)[\sqrt{s+R}\cosh(\sqrt{s+R}) + \alpha \sinh(\sqrt{s+R})]}$$

$$- \frac{RS}{s(s+R)} \quad (27).$$

By using the residue theory, the inverse Laplace transforms of $\bar{Y}(s)$ and $\bar{Y}(s,\lambda)$, $Y(\theta)$ and $Y(\theta,\lambda)$, are obtained as follows [see Appendix C]:

$$Y(\theta) = \frac{\alpha}{1+\alpha}\exp(-R\theta) - \sum_{n=1}^{\infty} \frac{2\exp(-(\beta_n^2+R)\theta)}{(1+\alpha+\frac{\beta_n^2}{\alpha})} - S(1-\exp(-R\theta)) \quad (28)$$

$$Y(\theta,\lambda) = \frac{\alpha}{1+\alpha}\exp(-R\theta) - \sum_{n=1}^{\infty} \frac{2\cos(\beta_n(1-\lambda))}{(1+\alpha+\frac{\beta_n^2}{\alpha})\cos\beta_n}\exp(-(\beta_n^2+R)\theta) \cdot$$

$$- S(1-\exp(-R\theta)) \quad (29)$$

These are the desired solutions.

It is seen that if $R = 0$, equations (28) and (29) become identical respectively with equations (13) and (14), the analytical solutions for the system with finite thickness of the packed bed and without chemical reaction. Figure 10 shows in dimensionless

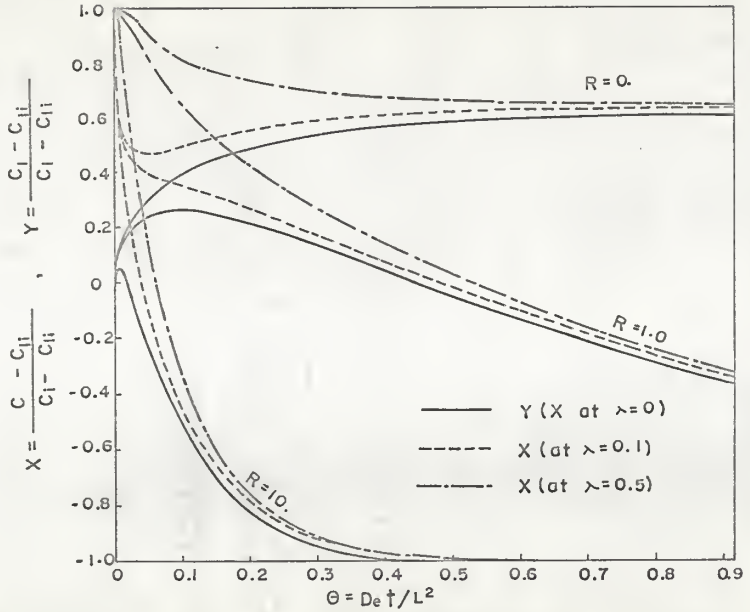

Fig. 10. Effect of the dimensionless reaction constant R on the concentrations X & Y when S = 1.0 & α = 1.77276 .

[illegible] concentration within the packed bed and in the well stirred reservior (identical with Y at λ = 0) change with respect to time for different values of the reaction constant, k (R includes k) when S = 1.0 and α = 1.77276. For α = 1.77276, β's are listed in Table 1. Because an irreversible first order reaction is applied in both layers, the concentration in the upper reservior increases until the diffusion process grows weak and chemical kinetics become dominant. At a position near the bottom, the concentration always decreases.

Figure 11 shows the concentration change vs. time for various values of λ and S when R and α are specified, for example, R = 1.0 and α = 1.77276. According to Figure 11, if time goes on to approach infinity, no matter what position may be considered, the concentration approaches -S asymptotically.

From equation (28), if α and S are specified, for instance, α = 1.77276 and S = 1.0, Y has a different profile for each value of R as θ varies. These profiles are shown in Figure 12. With experimental data and with equation (28) and Figure 12, the dimensionless reaction rate constant R can be obtained by forcing the experimental data to fit the theoretical solution. Once R has been obtained with known D_e, then the chemical reaction constant, k, can be calculated with ease.

CASE (III) : Diffusion with infinite thickness of the packed bed and without reaction

From the preceding chapter, the differential equations (6) and (7) are repeated below;

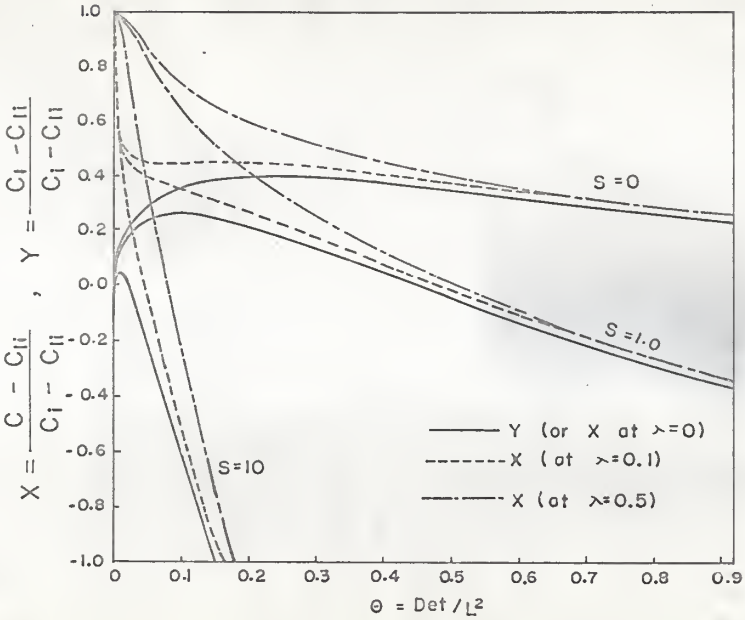

Fig. 11. Effect of the dimensionless initial concentration S on the concentrations X & Y when R = 1.0 & α = 1.77276.

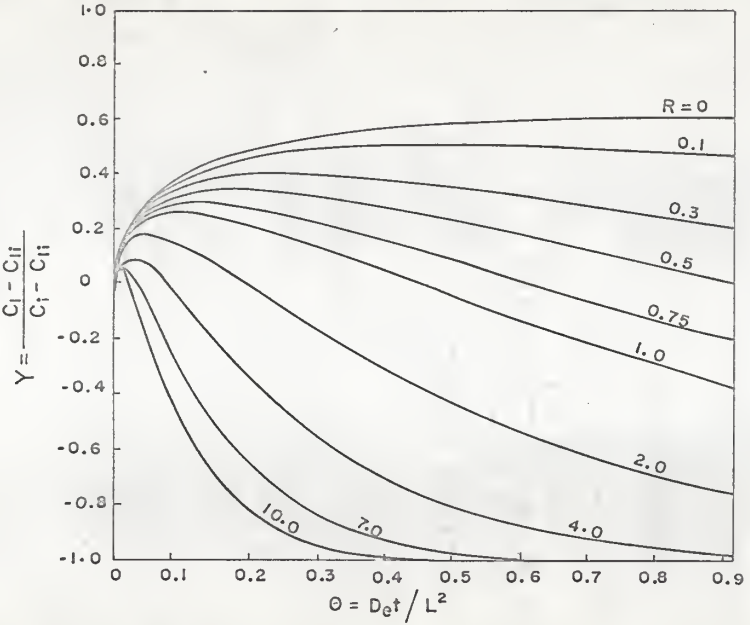

Fig. 12. Effect of the dimensionless reaction constant R on the upper reservoir's concentration when S=1.0 & α =1.77276.

$$\frac{\partial}{\partial} = D_{\epsilon} \frac{\partial^2 c}{\partial z^2} \tag{6}$$

and $$\frac{\partial c}{\partial z} = D \frac{\partial c}{\partial z}\Big|_{z=0} \quad \text{for } t > 0 \tag{7}$$

with initial and boundary conditions

(1) when $t = 0$,

$$c = c_i$$

and

$$c_1 = c_{1i},$$

(2) at $z = 0$,

$$c = c_1 \quad \text{for } t > 0,$$

and

(3) at $z = \infty$,

$$c = c_i.$$

For simplicity, the dimensionless group, equation (10.a), is introduced.

By substituting equation (10.a) into equations (6) and (7), the following equations are obtained.

$$\frac{\partial \nu}{\partial \theta_i} = \frac{\partial^2 \nu}{\partial \lambda_i^2} \tag{31}$$

$$\frac{\partial \nu}{\partial \theta_i} = \frac{\partial \nu}{\partial \lambda_i}\Big|_{\lambda_i=0} \tag{32}.$$

Using these dimensionless expressions, the initial and boundary conditions become

(1) when $\theta_i = 0$,

$$X = 1$$

and

$$Y = 0,$$

(2) at $\lambda_1 = 0$,

$$X = Y \quad \text{for } \theta_1 > 0,$$

and

(3) at $\lambda_1 = \infty$,

$$X = 1.$$

In order to solve this boundary values problem, Laplace transformation of equations (31) and (32) and the above initial and boundary conditions is carried out. Then

$$\frac{\partial^2 \overline{X}}{\partial \lambda_1^2} - s\overline{X} + 1 = 0 \tag{33}$$

$$\overline{Y} - \frac{1}{s} \frac{\partial \overline{X}}{\partial \lambda_1}\bigg|_{\lambda_1=0} \tag{34},$$

and transformed boundary conditions,

(1) at $\lambda_1 = 0$,

$$\overline{X} = \overline{Y}$$

and

(2) at $\lambda_1 = \infty$,

$$\overline{X} = \frac{1}{s}.$$

are obtained.

The general solution for equation (33) can be obtained with the above two boundary conditions and once $\overline{X}$ has been obtained as

a function of λ, $\overline{Y}$ can be obtained as a function of s as follows [Laplace Transformation]:

$$\overline{Y} = \left(\overline{Y} - \frac{1}{s}\right) \exp\left(-\lambda_1\sqrt{s}\right) + \frac{1}{s} \qquad (35),$$

$$\overline{Y} = \frac{1}{s(1 + \sqrt{s})} \qquad (36).$$

According to the Table of Inverse Laplace Transformation (11), the inverse Laplace transform of $\overline{Y}(s)$, $Y(\theta_1)$, is found in the following form:

$$Y(\theta_1) = 1 - \exp(\theta_1)\ \mathrm{erfc}(\sqrt{\theta_1}) \qquad (37).$$

By substituting equation (36) into equation (35) and by using the Table of Inverse Laplace Transformation (11), the inverse Laplace transform of $\overline{X}(s, \lambda_1)$, $X(\theta_1, \lambda_1)$, is obtained.

$$X(\theta_1, \lambda_1) = 1 - \exp(\theta_1+\lambda_1)\ \mathrm{erfc}\left(\sqrt{\theta_1} + \frac{\lambda_1}{2\sqrt{\theta_1}}\right) \qquad (38)$$

In equations (37) and (38), Y and X can be plotted with respect to θ_1 as shown in Figure 13, which can be compared with Figure 2. While the concentration at any point within the finite thickness of the packed bed approaches a final value, $\alpha/(1 + \alpha)$, as shown in Figure 2, that within the packed bed having infinite thickness approaches unity as shown in Figure 13. This is because of the fact that when the system has infinite thickness, the system has an infinite amount of substance to be diffused to the upper well stirred solution, whose volume is finite, until it has a uniform saturated concentration.

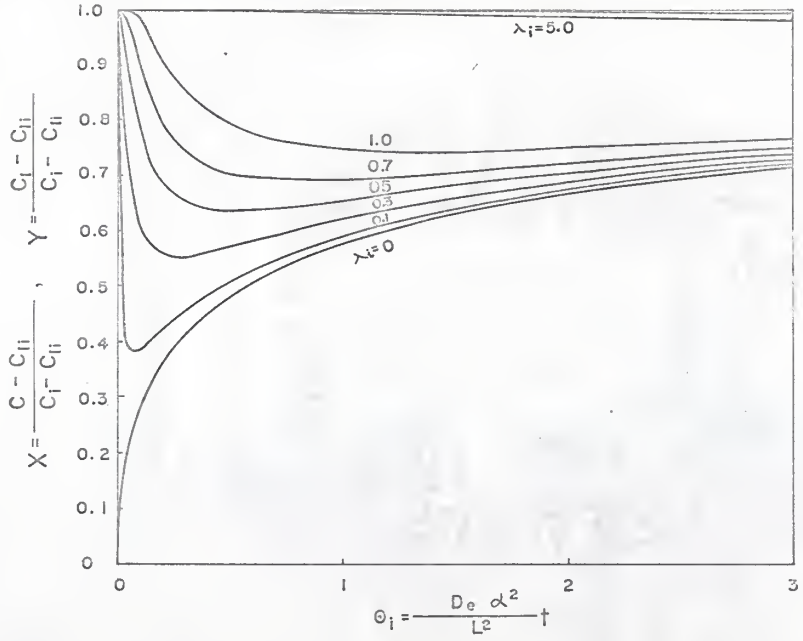

Fig. 13. Transient behavior of the concentrations X & Y (identical with X at $\lambda_i = 0$) in the semi-infinite packed bed system.

Figure 14, the plots of $\frac{c}{c_0}$ vs. Y vs. h_i, shows concentration profiles within the packed bed at different heights. The concentrations in the upper reservoir are shown by flat lines.

Case (IV) : Diffusion with infinite thickness of the packed bed and with an irreversible first order homogeneous reaction

For this case,

$$\frac{\partial c}{\partial t} = D_e \frac{\partial^2 c}{\partial z^2} - kc \qquad (8)$$

and $$V \frac{dc_1}{dt} = D_e \left.\frac{\partial c}{\partial z}\right|_{z=0} FA - Vkc_1 \quad \text{for } t > 0 \qquad (9),$$

are repeated with initial and boundary conditions

(1) When $t = 0$,

$$c = c_i$$

and

$$c_1 = c_{1i},$$

(2) at $z = 0$,

$$c = c_1 \quad \text{for } t > 0,$$

and

(3) at $z = \infty$,

$$c = c_i \exp(-kt)$$

or

$$\frac{dc}{dt} = -kc.$$

By substituting dimensionless group, equation (10.a), into equations

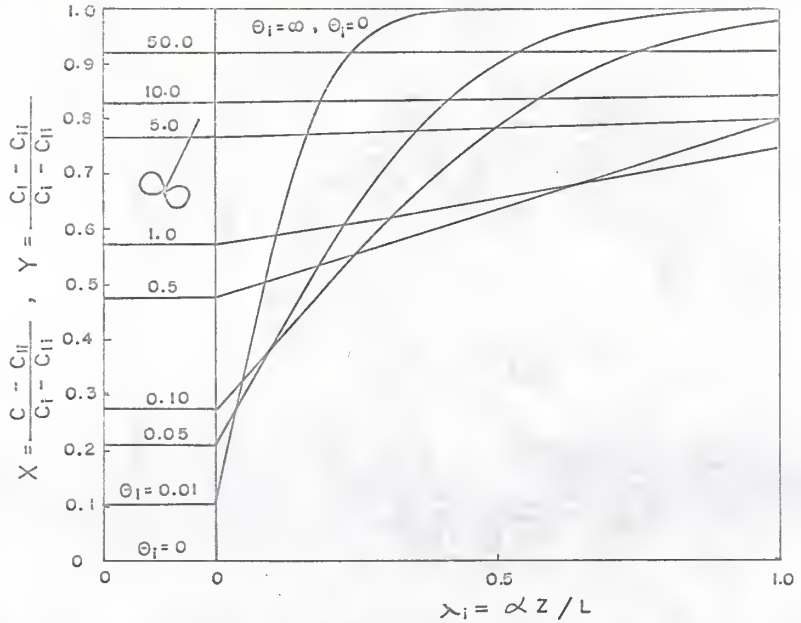

Fig. 14. Concentration profiles through the semi-infinite packed-bed.

(8) and (9),

$$\frac{\partial Y}{\partial \theta_i} = \frac{\partial^2 X}{\partial \lambda_i^2} - B_i (X + S_i) \qquad (39),$$

$$\frac{\partial Y}{\partial \theta_i} + B_i (Y + S_i) = \frac{\partial X}{\partial \lambda_i}\Big|_{\lambda_i = 0} \qquad (40)$$

are obtained where,

$$B_i = \frac{k V^2}{D_e P^2 A^2}$$

and

$$S_i = \frac{c_{1i}}{c_i - c_{1i}} .$$

If equation (10.a) is substituted into the initial and boundary conditions, then

(1) when $\theta_i = 0$,

$$X = 1$$

and

$$Y = 0,$$

(2) at $\lambda_i = 0$,

$$X = Y \quad \text{for } \theta_i > 0,$$

and

(3) at $\lambda_i = \infty$,

$$\frac{\partial Y}{\partial \theta_i} = - B_i (X + S_i)$$

are obtained.

By using the Laplace transformation, the analytical solutions for Y and X can be obtained as follows [see Appendix E]:

$$X(\theta_i) = \exp(-R_i\theta_i) - \exp[(1 - R_i)\theta_i]\,\mathrm{erfc}(\sqrt{\theta_i}) - S_i(1 - \exp(-R_i\theta_i)) \qquad (41),$$

$$X(\theta_i,\lambda_i) = \exp(-R_i\theta_i) - \exp[\lambda_i+(1-R_i)\theta_i]\,\mathrm{erfc}(\sqrt{\theta_i}+\lambda_i/2\sqrt{\theta_i}) - S_i(1 - \exp(-R_i\theta_i)) \qquad (42).$$

If $R_i = 0$, then equations (41) and (42) become identical with equations (37) and (38), the analytical solutions for the system with infinite thickness of the packed bed and without reaction. Figure 15 shows in dimensionless form how the concentrations within the packed bed and in the well stirred reservoir (equal to X at $\lambda_i = 0$) vary with respect to time at different positions within the packed bed for various values of the dimensionless reaction constant R_i when $S_i = 1.0$. If $R_i = 0$, this figure becomes identical to Figure 13.

Figure 16 shows the concentration change vs. time for various values of λ_i and S_i when $R_i = 1.0$. It is seen in Figure 16 that as time goes on to reach infinity regardless of the position, the concentration approaches $-S_i$ asymptotically.

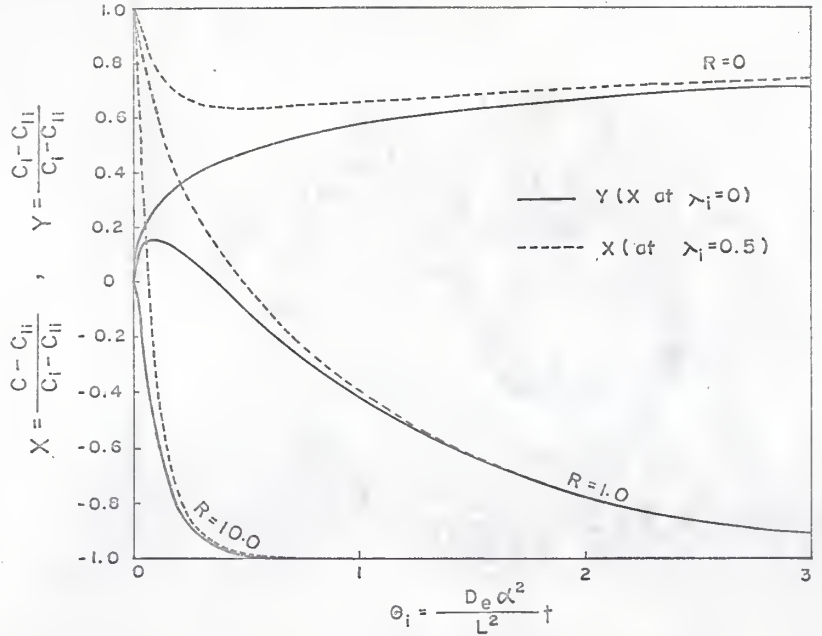

Fig. 15. Effect of the dimensionless reaction constant R_1 on the concentrations X & Y (identical with X at $\lambda_i=0$) when $S_1=1.0$.

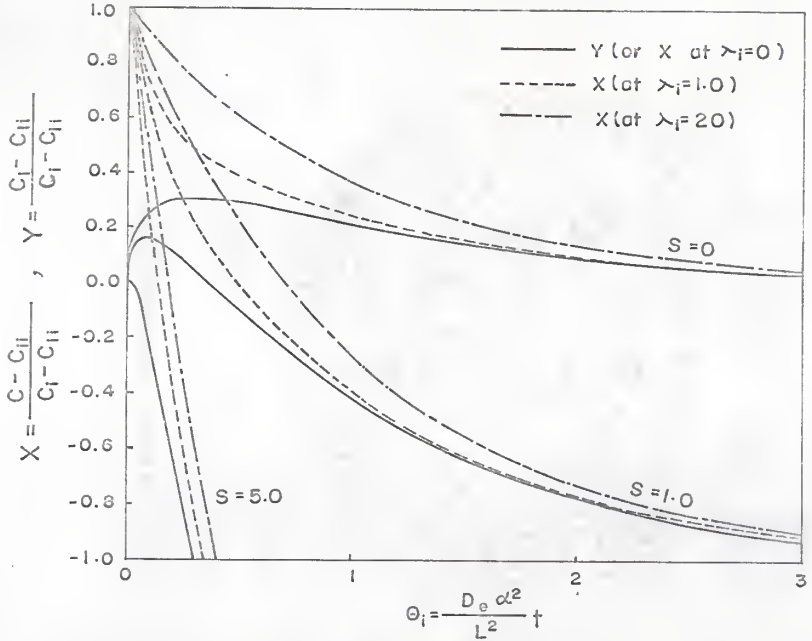

Fig. 16. Effect of the dimensionless initial concentration S_i on the concentrations X & Y (identical with X at $\lambda_i = 0$) when $R_i = 1.0$.

CHAPTER IV

EXPERIMENT WITH AQUEOUS SUCROSE SOLUTION

For the purpose of testing and calibrating the experimental set-up shown in Figure 17, which simulates the system under consideration, diffusion experiments were carried out by using an aqueous sucrose solution for which the diffusivity was known. These experiments enabled us to verify the mathematical expressions obtained in the previous chapters, and more specifically enabled us to determine the ranges of experimental condition for which the system equations are valid.

EXPERIMENTAL EQUIPMENT

The apparatus used for conducting the diffusion experiments consisted of a packed bed and a well stirred reservoir as shown in Figure 17. For this system two lucite cylinders, 10.716 cm ID and 19.65 cm inside depth and 10.716 cm ID and 33.2 cm long, for the packed bed and the well stirred reservoir respectively, were prepared and connected together by flanges.

To keep the upper reservoir at a uniform concentration for a given time, it was agitated by a stirrer operated by a motor which was controlled from a variable autotransformer powerstat. To prevent up-down flow, the stirrer selected was of the multiple flat-blade turbine type instead of the propeller type.

To prevent up-down bulk flow and moving particles, two sheets of 250 mesh stainless steel screen were installed between the packed bed and the well stirred reservoir. As inert particles,

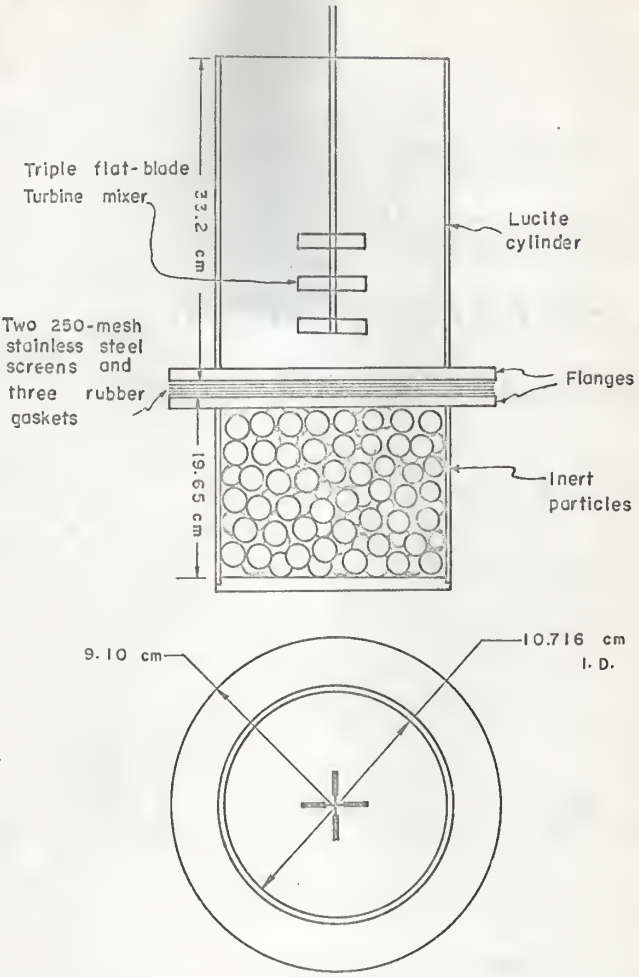

Fig. 17. Schematic diagram of the experimental set-up.

25 — 30 mesh glass beads and 65 — 80 mesh glass typers were used.

To analyse the sucrose sample solutions taken from the upper reservoir, a Bausch & Lomb refractometer was used for measuring their concentrations by referring to the regractive index of sucrose solution listed in the International Critical Tables (14).

EXPERIMENTAL PROCEDURES

In a typical experimental run, the packed bed was saturated with an aqueous sucrose solution and in contact with a well stirred solution in the upper reservoir. Because the density of sucrose solution increases with its concentration, the concentration of the upper well stirred solution should be lower than that of the solution within the packed bed. This prevented bulk flow across the screens by gravitational force.

In order to diminish the effect of the agitating motion on bulk flow across the screens, the speed of the agitating motor was set as low as possible within the range so that the upper solution was able to maintain a uniform concentration at any time while an experimental run was proceeding. The upper reservoir could be checked for uniformity of concentration. That is, sample solutions were caught at two positions, at 3.5 cm below the surface of the well stirred solution and at 3.5 cm above the upper screen.

In analysing the sample solutions by the Bausch & Lomb refractometer, only 1 — 2 ml of the upper reservoir's solution was needed. To lessen the error from volume change of the upper

solution when a sample was taken, an equal amount of solution whose concentration was identical to the previous sample was poured back into the reservoir.

The Bausch & Lomb refractometer was calibrated as shown in Figure 18 and Table 2. From Table 2, the following relation between x and y can be obtained:

$$y = 0.9899\ x - 0.01238 \qquad (43).$$

When sample solutions were taken and their concentrations measured, a temperature correction was necessary because the refractive index of the sucrose solution was sensitive to the temperature of the circulating water of the Bausch & Lomb refractometer. For this refractometer, a temperature correction table was made for the deviation from the standard temperature (20 ^{o}C) as shown in its manual (19). Once the concentration of a sample sucrose solution was measured by the refractometer, the real concentration of the solution could be calculated according to the calibtation equation, equation (43). The molar concentration of the solution was obtained from the weight % concentration by using the Table of Density of Aqueous Sucrose solution in the International Critical Tables (14).

Under these considerations, experiments were performed for four different conditons listed in Table 3. For each run, sample solutions were caught only from the well stirred reservoir.

EXPERIMENTAL RESULTS AND DISCUSSIONS

The experimental data obtained under the experimental

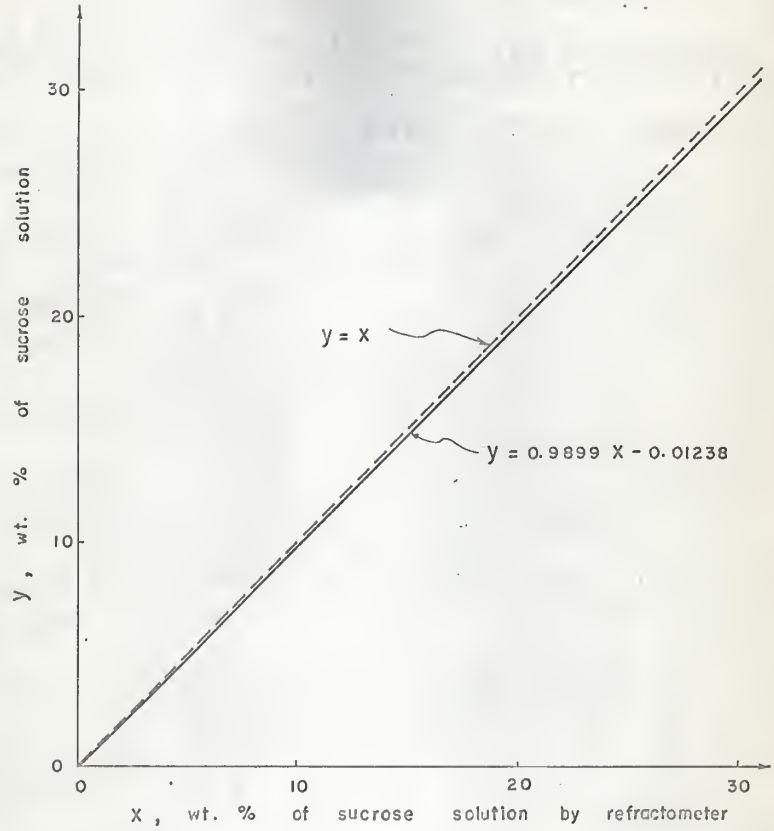

Fig. 18. Calibration of the Bauseh & Lomb refractometer.

Table. 2. Calibration of the Bausch & Lomb refractometer.

concentrated sucrose solution		dilute sucrose solution	
real weight % (y)	weight % by regractometer (x)	real weight % (y)	weight % by refractometer (x)
30.21	30.55	9.054	9.194
	30.60		9.124
	30.43		9.154
	avg. 30.53		avg. 9.157

Table. 3. Experimental conditions

run number	3	5	6	8
interfacial area (cm^2)	90.217	90.217	90.217	90.217
size of inert particle (mesh No.)	65 - 80 glass tyler	65 - 80 glass tyler	25 - 30 glass bead	25 - 30 glass bead
porosity of packed-bed	0.3655	0.3655	0.3582	0.3582
packed-bed length (cm)	19.65	19.65	19.65	19.65
upper reservoir's volume (cm)	1500	1500	1500	1500
RPM of agitating motor	75 - 80	75 - 80	75 - 80	750
initial Conc. in upper reservoir (g-moles/l)	0.3098	0.2818	0.3182	0.3785
initial Conc. within packed-bed (g-moles/l)	1.0148	0.9492	0.6874	0.8622
room temperature (^oC)	22 -26	22 - 26	20 - 25	18 - 23

conditions given in Table 3, which are the concentrations of the sample solutions taken from the upper well stirred reservoir, are listed in Table 4 for Run (3), in Table G-4 for Run (5), in Table G-5 for Run (6), and in Table G-6 for Run (8). These data were corrected for temperature deviation.

One of the factors, which caused the rise of the initial concentration in the upper well stirred solution appeared to be the initial disturbance which might exist when the upper solution contacted the packed bed. In other words, even though it was small, there existed bulk flow across the screens when both solutions were brought in to contact. This bulk flow might give rise to radial and axial concentration gradients near the interface within the packed bed. The agitating motion which kept the upper reservoir at a uniform concentration also must have affected the packed bed by inducing the convective motion. The initial penetration (or disturbance) and the continuous convective motion of the fluid must affect the system in a very complex fashion. It is very difficult, if not impossible, to analyze these complex effects. Preliminary investigation indicated that a single correction factor, i.e., the depth correction factor which reduces the effective thickness of the packed bed and increases the volume and the initial concentration of the upper solution, might satisfactorily correct for those disturbances. The corrected thickness of the packed bed L_c and the corrected volume and initial concentration of the upper solution, V_c and c_{lci}, change according to this depth correction factor L_o.

In order to determine this factor, a one dimensional search

Table. 4. Experimental data for Run (3)

L_o = 1.0037 cm

c_{1ci} = 0.32502 moles/liter

time (hrs)	position H:high L:low	refractive index	wt % conc.	temp. (°C)	temp. correction (wt %)	wt % by refracto-meter	real wt %	molar conc. (moles/l)	average molar conc. (moles/l)	corrected dimensionless conc., Y_c
4	H	1.34860	10.55	22.60	0.18	10.72	10.60	0.3223	0.3221	-0.004232
		1.34875	10.60	22.60	0.18	10.78	10.66	0.3242		
	L	1.34856	10.50	22.50	0.18	10.68	10.56	0.3210		
		1.34855	10.50	22.50	0.18	10.68	10.56	0.3210		
14	H	1.34880	10.67	22.60	0.18	10.85	10.73	0.3264	0.32615	0.001639
		1.34885	10.68	22.60	0.18	10.86	10.74	0.3267		
	L	1.34875	10.60	22.60	0.18	10.78	10.66	0.3242		
		1.34890	10.70	22.60	0.18	10.88	10.76	0.3273		
16	H	1.34890	10.70	22.70	0.19	10.89	10.77	0.3276	0.3276	0.003741
		1.34890	10.70	22.70	0.19	10.89	10.77	0.3276		
	L	1.34890	10.70	22.70	0.19	10.89	10.77	0.3276		
		1.34890	10.70	22.70	0.19	10.89	10.77	0.3276		
18	H	1.34900	10.70	22.75	0.19	10.89	10.77	0.3276	0.32795	0.004249
		1.34930	10.72	22.75	0.19	10.91	10.79	0.3283		
	L	1.34890	10.70	22.70	0.19	10.89	10.77	0.3276		
		1.34892	10.72	22.75	0.19	10.91	10.79	0.3283		
21	H	1.34940	11.00	19.00	-0.06	10.94	10.82	0.3292	0.32905	0.005843
		1.34940	11.00	19.00	-0.06	10.94	10.82	0.3292		
	L	1.34940	11.00	19.00	-0.06	10.94	10.82	0.3292		
		1.34940	10.98	19.00	-0.06	10.92	10.80	0.3286		

Table. 4. Experimental data for Run (3)(continued)

L_o = 1.0037 cm

c_{lci} = 0.32502 moles/liter

Time (hrs)	position H:high L:low	refractive index	wt % conc.	temp. (°C)	temp. correction (wt %)	wt % by refracto-meter	real wt %	molar conc. (moles/l)	average molar conc. (moles/l)	corrected dimensionless conc., Y_c
	H	1.34940	11.01	19.40	-0.04	10.97	10.85	0.3302	0.3301	0.007366
		1.34940	11.01	19.40	-0.04	10.97	10.85	0.3302		
	L	1.34935	10.98	19.40	-0.04	10.94	10.82	0.3292		
		1.34945	11.03	19.40	-0.04	10.99	10.87	0.3308		
	H	1.34925	10.95	21.00	0.07	11.02	10.90	0.3336	0.3329	0.011420
		1.34920	10.91	21.10	0.08	10.99	10.87	0.3308		
	L	1.34925	10.95	21.00	0.07	11.02	10.90	0.3336		
		1.34925	10.95	21.00	0.07	11.02	10.90	0.3336		
	H	1.34950	11.10	21.05	0.07	11.17	11.04	0.3362	0.3359	0.015770
		1.34945	11.05	21.00	0.07	11.13	11.00	0.3350		
	L	1.34950	11.10	21.00	0.07	11.17	11.04	0.3362		
		1.34950	11.10	21.00	0.07	11.17	11.04	0.3362		
	H	1.34940	11.00	22.50	0.18	11.18	11.05	0.3365	0.33668	0.016900
		1.34943	11.03	22.50	0.18	11.21	11.08	0.3375		
	L	1.34950	11.10	21.00	0.07	11.17	11.04	0.3362		
		1.34940	11.00	22.50	0.18	11.18	11.05	0.3365		
	H	1.34938	11.00	22.50	0.18	11.18	11.05	0.3365	0.33675	0.017010
		1.34930	10.97	22.70	0.19	11.16	11.03	0.3359		
	L	1.34945	11.05	22.50	0.18	11.23	11.10	0.3381		
		1.34940	11.00	22.50	0.18	11.18	11.05	0.3365		

technique (Golden Section method) was applied so that the sum of the square deviations might be minimized. That is, L_o was searched to minimize

$$E = \sum_{1}^{m}(Y_c - Y_e)^2 \tag{44}$$

where E = sum of the square deviations,

m = number of data,

Y_c = corrected theoretical value, and

Y_e = corrected experimental value.

In this case, Y_c was obtained by modifying equation (16) to the form of the following equation.

$$Y_c = \frac{1}{1 + \frac{V_c}{AL_cP}} - \sum_{n=1}^{\infty} \frac{2}{1 + \frac{AL_cP}{V_c} + \frac{V_c\beta_n^2}{AL_cP}} \exp\left(-\frac{\beta_n^2 D_e}{L_c^2} t\right) \tag{45}$$

where

$$L_c = L - L_o$$

$$V_c = V + AL_oP.$$

And β_n is one of the eigenvalues which satisfy the following eigenfunctions. Since $\alpha = 0.43196$ for Runs (3) and (5), the eigenfunction is

$$\beta \cot\beta + 0.43196 = 0 \tag{46}.$$

Similarly, since $\alpha = 0.42334$ for Runs (6) and (8), the eigenfunction is

$$\beta \cot\beta + 0.42334 = 0 \tag{47}.$$

Two sets of the first twenty eigenvalues which satisfy equations (46) and (47) are listed in Table 5. The effective diffusivity, D_e, is defined as [see equations (1) and (3)]

$$D_e = \frac{D_o}{T}$$

Here, T was chosen to be $\sqrt{2}$ as suggested by Penman (17) and Carman (18). The molecular diffusivity, D_o, of sucrose in aqueous solution was taken as 4.242×10^{-6} cm^2/sec (14, 15, 16). Thus, the effective diffusivity of aqueous sucrose solution, D_e, was computed to be 3.0×10^{-6} cm^2/sec.

For a known value of effective diffusivity, Y_c is a function of depth correction factor L_o and time t.

The corrected dimensionless experimental value of concentration, Y_e, is obtained from the equation

$$Y_e = \frac{c_{le} - c_{lci}}{c_i - c_{lci}} \tag{48}$$

where

c_{le} = experimental value of c_l

c_{lci} = corrected value of c_{li}.

c_{lci} is given by

$$c_{lci} = \frac{Vc_{li} + AL_oPc_i}{V + AL_oP} \tag{49}$$

Accordingly, Y_e is a function of L_o for a given value of t.

Hence, by substituting equations (45), (48) and (49) into equation (44), it can be shown that the sum of square deviations,

Table. 5. Two sets of eigenvalues from equations (46) and (47).

eigen-values	for Run (3) and (5)	for Run (6) and (8)
β_1	1.80554	1.80206
β_2	4.80199	4.80053
β_3	7.90838	7.90751
β_4	11.03456	11.03384
β_5	14.16772	14.16714
β_6	17.30378	17.30320
β_7	20.44160	20.44107
β_8	23.58030	23.57990
β_9	26.72003	26.71965
β_{10}	29.85969	29.85933
β_{11}	32.99979	32.99952
β_{12}	36.14022	36.14000
β_{13}	39.28094	39.28065
β_{14}	42.42166	42.42145
β_{15}	45.56252	45.56238
β_{16}	48.70348	48.70338
β_{17}	51.84458	51.84439
β_{18}	54.98568	54.98561
β_{19}	58.12638	58.12669
β_{20}	61.26818	61.26792

E, is a function of the depth correction factor L_o for given values of D_e and t. That is, equation (44) can be rewritten as

$$E(L_o) = \sum_{1}^{m} (Y_c(L_o) - Y_e(L_o))^2 \qquad (50).$$

As described above, the one dimensional Golden Section method was used to search the depth correction factor L_o such that the sum of square errors E might be minimized. The computer flow chart and program for this method are listed in Appendix (G).

To examine the accuracy of each experimental run, the standard deviation (23) is obtained by the equation

$$\sigma = \sqrt{\frac{E}{n}} \qquad (51).$$

For Runs (3), (5) and (6), the depth correction factors were found to be 1.0037, 0.6958 and 3.4874 cm respectively as shown in Figure 19. The standard deviations for those cases were 3.678×10^{-3}, 3.006×10^{-3} and 1.863×10^{-3} respectively. According to Figure 19, the system having a packed bed composed of small inert particles had a low value of depth correction while the system having a packed bed composed of large inert particles had a greater value. This could have been because the former bed was more compact than the latter.

For each of these correction factors, the corrected experimental data are listed in Table 4 for Run (3), and in Tables G-4 and G-5 for Runs (5) and (6) respectively. The data from Runs (3), (5) and (6) are plotted in Figure 20.

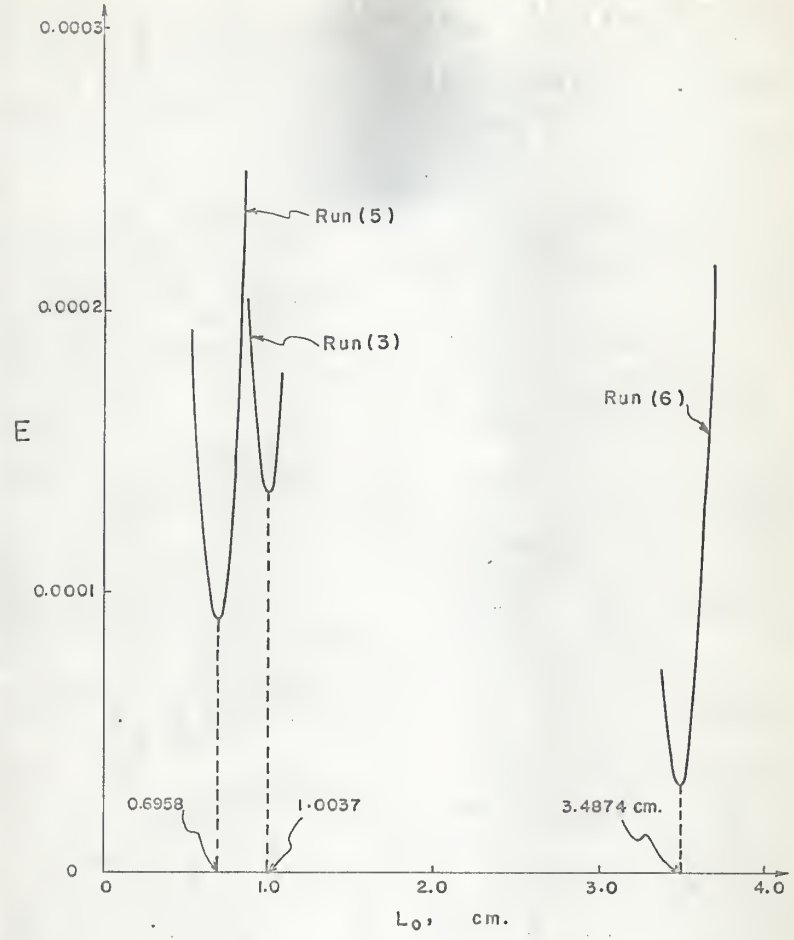

Fig. 19. Determination of depth correction factors.

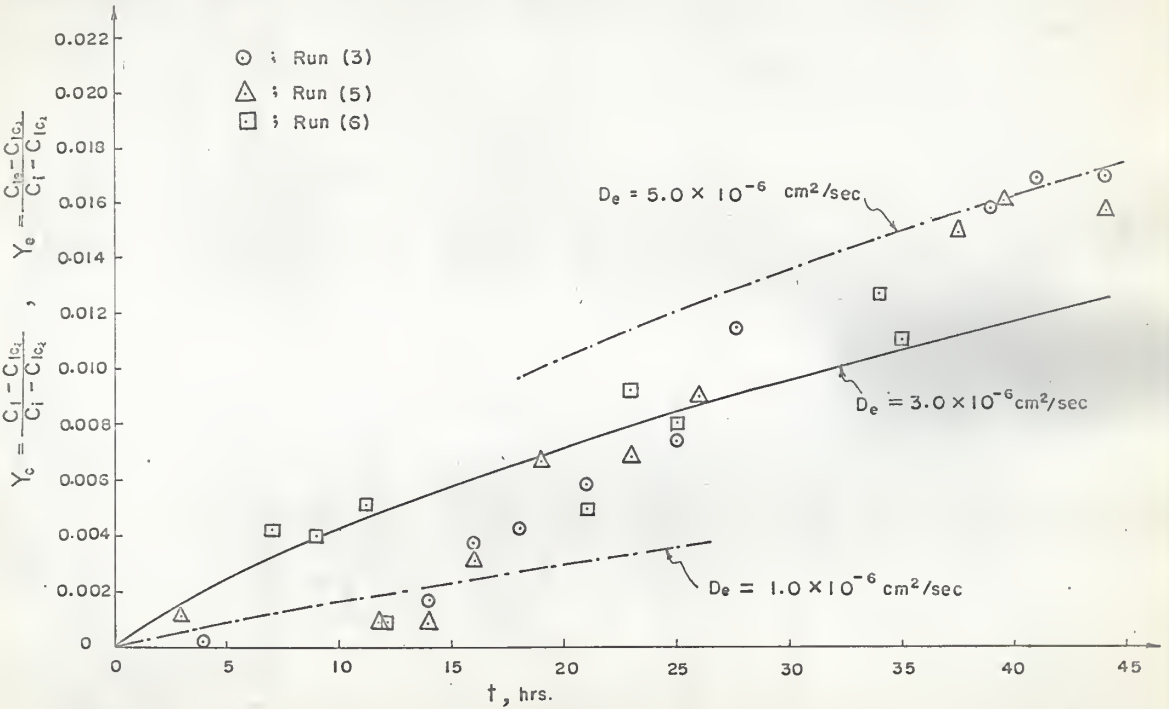

Fig. 20 Corrected theoreticol & experimental concentrotions Y_c & Y_e vs. t for Runs (3), (5) & (6).

For the first period up to about 25 hours, the concentrations in the upper reservoir obtained by experiments were smaller than those obtained by the theoretical equation with an average value of effective diffusivity of sucrose solution (3×10^{-6} cm^2/sec). In other words, for the first 25 hours the diffusivity of the aqueous sucrose solution measured by experiment was less than the average value of the available data, while after this period it was greater than the average. This might possibly be explained as follows: Generally, the diffusivity of sucrose has not been considered constant but has been considered as a function of the concentration of the solution. According to International Cririca1 Tables (14), Henrion (15) and Van Hook (16), the diffusivity of aqueous sucrose solution decreases as its concentration increases.

Initially the concentration of the packed bed was high and it became low as the diffusion process was proceeding. Thus, the effective diffusivity of the aqueous sucrose solution through the packed bed was initially small and became larger gradually, up to a certain value. As previously mentioned, a single correction factor in terms of the depth correction factor was employed to take into account the effects of disturbances due to such factors as the initial penetration and the continuous convective motion in the bed. This factor changed the relative sizes of the thickness of the bed and the upper reservoir's volume. Since the conditions in the system, or more specifically the concentration profile in the system, changed with respect to time, the use of the single correction factor could not correct uniformly for

those disturbances from the onset of the process to the end of the process. Since the correction factor was determined for the whole range of the process, this overall or average correction factor might overcorrect the data from the initial part of the process and undercorrect the data from the later part of the process.

However, the diffusivity obtained here was not out of the range of its known values. The measured diffusivities of aqueous sucrose solutions have been in the range of $1.5 - 7.0 \times 10^{-6}$ cm^2/sec at temperatures of less than 25 °C (14, 15, 16). Accordingly, the effective diffusivities, which are the values of true diffusivities divided by the approximate tortuosity $\sqrt{2}$, were in the range of $1.0 - 5.0 \times 10^{-6} cm^2/sec$.

As listed in Table 3, for Runs (3), (5) and (6), the RPM of the agitating motor was in the range of 75 - 80. To check if the upper solution had a uniform concentration, sample solutions were arbitrarily taken both at the position of 3.5 cm below the surface of the upper solution and at the position of 3.5 cm above the upper screen. The concentrations at each of the points divided by their average were plotted in Figure 21, which showed that with 75 - 80 RPM of the agirating motor, the upper solution had uniform concentration in the reservoir.

To find the effect of large RPM of the agitating motor, Run (8) was carried out. In this situation, the effect of agitation was so large that equation (45) could not be used without adding another correction factor. Assuming that the effect of the agitating motor increases the effective diffusivity, the modified

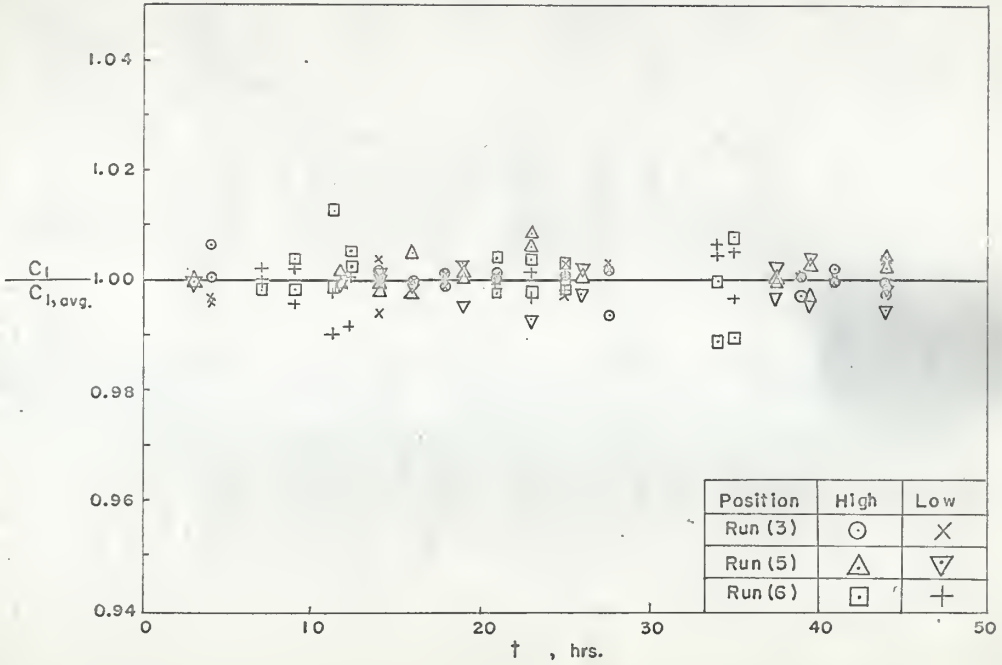

Fig. 21. Normalized concentrations at each sampling time.

effective diffusivity, K, defined below can be used in equation (45).

$$K = D_e + \pi \qquad (52)$$

where,

D_e = effective diffusivity of a substance (in this case, sucrose) in the solution

π = effect of agitating motor expressed in diffusivity units.

Then, the sum of square errors E should also be rewritten as follows:

$$E = \sum_{1}^{m} (Y_c(K, L_o) - Y_e(L_o))^2 \qquad (53).$$

It was shown that this is a two dimensional search problem for K and L_o. By using the Box method, the computer program of which is listed in Chen's thesis (24), K and L_o were obtained to be 9.428×10^{-5} cm^2/sec and 0.7657 cm respectively as shown in Figure G-2 and Table G-3 in Appendix (G). The standard deviation was 3.634×10^{-3}. The data for Run (8) were shown in Figure 22.

CONCLUSIONS

An experimental set-up which simulates the diffusion process of COD through a porous stratum saturated by water was proposed. The experimental set-up was tested and characterized by the experiments with sucrose solution whose diffusivity was known.

One single correction factor was suggested in terms of the depth correction factor to take into account the effects of

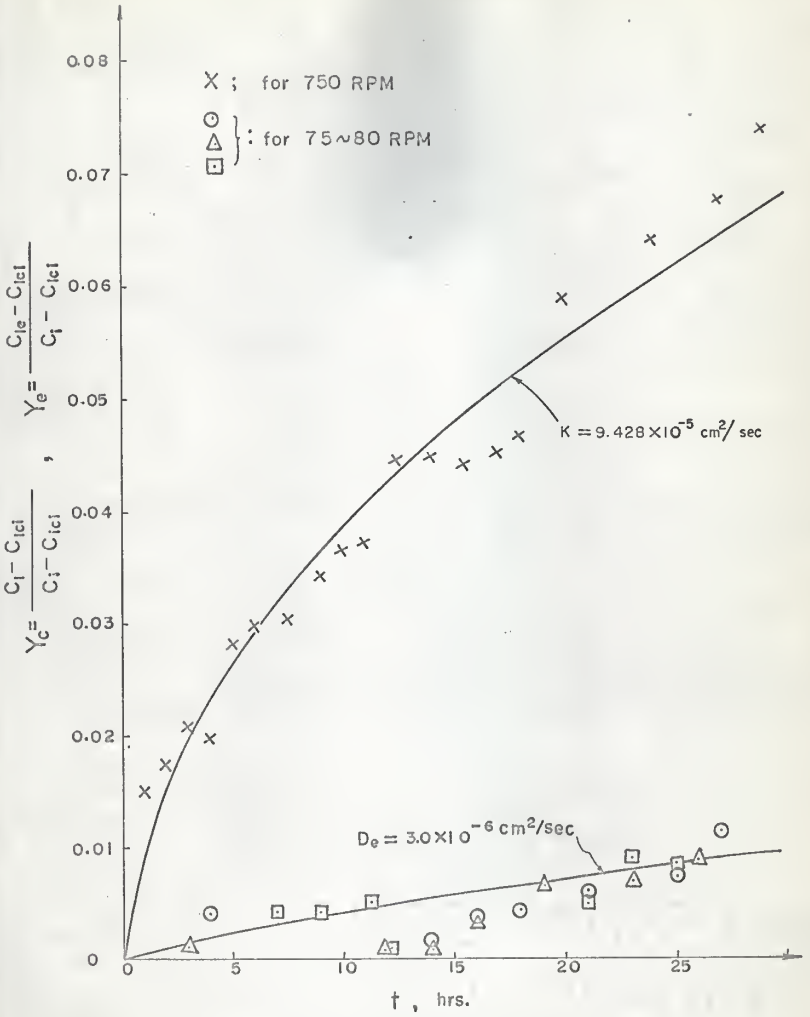

Fig. 22. Effect of speed of agitating motor.

disturbances such as the initial penetration of the upper solution and the continuous convective motion in the bed. It was found to be 0.84975 cm. It was also found that the speed of the agitation motor should be maintained within a limit of 75 — 80 RPM.

It can be concluded that this experimental set-up can be used as one of the simplest and quickest methods to determine the diffusivity of a substance in water with reasonable accuracy.

CHAPTER V

TRANSPORT RATE OF COD BY DIFFUSION THROUSH A POROUS PACKED BED SATURATED BY WATER

The experiments with feedlot runoff were carried out by using the system which was tested and calibrated in the previous chapter. Feedlot runoff contains a complex mixture of many components. For simplicity, it was decided to consider it as a hypothetical binary mixture. One component of this hypothetical binary mixture is the dissolved organic matter which is measured by the COD test, and the other the remaining materials. As previously mentioned, since COD was assumed to use as a hypothetical compound, the diffusivity of COD in feedlot runoff then is the overall or average diffusivity of various types of organic matter in the feedlot runoff, which may be called "pseudo-molecular diffusivity". As mentioned in the previous chapters, the so-called effective diffusivity of a substance characterizes the diffusivity through the porous packed bed which includes the tortuosity effect. Then the effective pseudo-diffusivity D_{pe} of COD in feedlot runoff through a porous medium can be related as follows; that is,

$$D_{pe} = \frac{D_p}{T} \tag{54}$$

where

D_p = pseudo-diffusivity (or pseudo-molecular diffusivity) of COD which represents the overall molecular diffusivity of various types of organic matter, cm^2/sec

D_{pe} = effective pseudo-molecular diffusivity of COD though the porous packed bed, cm^2/sec

T = tortuosity of the packed bed.

The effective pseudo-diffusivity of COD can be obtained by using the system described in the foregoing chapters.

The experimental condition was the same as that of Runs (3) and (5) in which sucrose solution was used; thus, the calibration made with use of sucrose solution remained valid for the experiments with feedlot runoff.

EXPERIMENTAL

(A) Equipment

The equipment which had been used in the previous experiments with sucrose solution was used again here except for the Bausch & Lomb refractometer. To determine the COD concentration, the standard method (20) was used. Reflux apparatus consisted of a 300 ml round-bottom flask (Corning No. 4320 or equal) with ground glass neck 24/40 and a Friedrichs condenser (Corning No. 2600 or equal). Reagents employed were standard potassium dichromate solution (0.250 N), concentrated sulfuric acid, standard ferrous ammonium sulfate solution (0.25 N) and ferroin indicator solution.

(B) Procedures

(1) Preparation of Cattle Manure Solution

To prepare the cattle manure solution for use in the experiments, cattle manure was taken from the cattle feedlot located in the northern part of the campus of Kansas State University. This

manure was saturated with a large amount of water for two or three days. During this period, it was agitated a few times. After settling two days, the upper solution was taken and filtered with a sheet of filter paper. The fitrate was filtered again to remove even small manure particles.

Before this manure solution was used as an original waste water, it was necessary to make sure that no micro-organisms existed to reduce the COD concentration by consuming organic matter. To do this, the original waste water was heated at the temperature range of 120 — 150 ^{o}C for 1.5 — 2 hours. A chemical also could have been used to kill the micro-organisms, but it is difficult to assure that it does not affect the COD of the solution after killing the micro-organisms. Moreover, unless oxygen is supplied to the waste water, the oxidation by micro-organisms can be neglected. In this preparation, a heating method like that used in daily milk production was introduced.

As references, the typical daily manure production of a 1000 pound steer on full feed and the analytical results of feedlot runoff which had been obtained by Miner (4) are listed in Tables 6 and 7.

(2) Standard Method for Determining COD

The method of determining COD was mentioned in Standard Methods for the Examination of Water and Wastewater (20). According to this method, 0.250 N of potassium dichromate solution and 0.25 N of ferrous ammonium sulfate solution are the oxidizing and reducing agents respectively. The reducing agent was standardized against the oxidizing agent as follows:

Table. 6. Typical Daily Manure Production of a 1000 pound Steer on Full Feed (4).

	Manure	Feces	Urine
Wet wt. (lbs.)	64	48	16
Dry wt. (lbs.)	10	9.5	0.5
Volatile solids (lbs.)	8		
BOD (lbs.)	1.3		
COD (lbs.)	13		
Nitrogen (lbs.)	0.39	0.18	0.21
Potassium (lbs.)	0.3		
Phosphorous (lbs.)	0.05		

Table. 7. Analytical Results - General Runoff Samples (4).

Sample No.	0625A	0625L	0626A	0626B	0626L	0626M	0701A	0703A	0703L
COD	12,600	17,100	32,700	12,600	12,600	6,800	15,200	16,700	8,050
BOD	1,350	1,050	3,500	950				1,460	530
Nitrogen									
Kjeldahl	645	246	410	240	214	88	915	750	415
Ammonia	120	55	310	119	123	55	91	104	2
Nitrite	10	4	12	9	3	3		6	2
Nitrate	8	7	--	14	17	8	6	6	
Suspended slds.									
Total	9,000	3,300	23,000	5,040					
Volatile									
Nonvolatile									
Turbidity No.									
Chloride	850	520	1,180	115	815	300		540	400
Phosphate	250	120	25	120	40	25		80	45
Lignin	320	120	430	270	200	80	220	220	90
PH	8.7	8.6	8.3	7.9	8.3	7.9			
Coliform									
Total	2.4	24	4.9	24			3.3	24	34.8
Fecal	2.4	24	4.9	24			3.3	24	34.8
Fecal Strep.	2.4	24	7.9	24			3.3	7.9	13.0
Lot condition	D	D	D	D	D	D	D	W	W

* Note; D = Dry
W = Wet

$$\text{Normality} = \frac{(\text{ml } K_2Cr_2O_7)\ (0.25)}{\text{ml } Fe(NH_4)_2(SO_4)_2} \qquad (55).$$

Because the COD test is designed to measure the oxygen requirement by oxidation of the organic matter present in the sample, it is important that no organic matter from outside sources appears in the sample during the test. Therefore, it is recommended that a parallel blank sample is tested.

If standard reagents as mentioned above are used, the COD of a sample solution can be computed as follows:

$$\text{COD (mg/l)} = \frac{(u - v)(w)(8000)}{\text{ml sample}} \qquad (56)$$

Where

u = ml $Fe(NH_4)_2(SO_4)_2$ used for blank

v = ml $Fe(NH_4)_2(SO_4)_2$ used for sample

w = normality $Fe(NH_4)_2(SO_4)_2$.

Here, the correction for the chloride interference was neglected.

(3) Procedures

The experimental procedures were almost the same as those in the case of sucrose solution, which were described in the preceding chapter, except for the method of determining the COD concentration.

Water was used as an original upper solution and the cattle manure solution mentioned in the foregoing subsection was used as an original solution for saturating the lower packed bed.

Twenty five ml of the solution were needed to determine the COD concentration of the solution taken from the upper reservoir.

To reduce the error caused by decreasing the volume of the upper reservoir, the same amount of solution (25 ml) with a concentration equal to that of the previous sample was poured back into the reservoir.

Two experiments were carried out under the different initial conditions given in Table 8.

EXPERIMENTAL RESULTS AND DISCUSSIONS

The experimental data obtained are listed in Tables 9 and 10 for experimental Runs (11) and (12) respectively. The values of the effective pseudo-diffusivity of COD were determined by forcing the experimental data to fit the mathematical expression. The conventional least square criterion as given by equation (44) in the preceding chapter was used. For convenience, equation (44) is repeated below:

$$E = \sum_{1}^{\infty} (Y_c - Y_e)^2 \qquad (44)$$

where

Y_c satisfies the modified equation (45)

$$Y_c = \frac{1}{1+\frac{V_c}{AL_cP}} - \sum_{n=1}^{\infty} \frac{2}{1+\frac{AL_cP}{V_c}+\frac{V_c\beta_n^2}{AL_cP}} \exp\left(-\frac{\beta_n^2 D_{pe}}{L_c^2} t\right) \qquad (45.a)$$

and Y_e represents the dimensionless experimental data defined in equation (48). Y_c is a function of the effective pseudo-diffusivity D_{pe}. To compute Y_c's, the eigenvalues β_n's which satisfy equation (15) in Chapter III are needed. $\alpha = 0.40571$

Table. 8. Experimental conditions for cattle manure

run number	11	12
interfacial area (cm^2)	90.217	90.217
size of inert particles (mesh No.)	65 - 80 glass tyler	65 - 80 glass tyler
porosity of packed-bed	0.3655	0.3655
packed-bed thickness (cm)	19.65	19.65
upper reservoir's volume (cm^3)	1500	1500
RPM of agitating motor	75 - 80	75 - 80
initial conc. in upper reservoir (mg/liter)	0	0
initial conc. within packed-bed (mg/liter)	6966	2998
room temperature (^oC)	23 - 27	23 - 26
note	original manure solution was used without heat treatment	original manure solution was treated by heat for 2 hours at 140 ^oC

Table. 9. Experimental data for Run (11)

L_o = 0.84975 cm
c_{lci} = 127.74 mg/liter

kind of sample (hrs)	volume of sample (cm^3)	volume of $K_2Cr_2O_7$ (cm^3)	boiling time (hrs)	volume of $Fe(NH_4)_2(SO_4)_2$ (cm^3)	normality	COD (mg/liter)	corrected dimensionless concentration Y_e
blank		25	1	25.65	0.2436		
5	25	25	1	23.11	0.2436	198	0.010275
17	25	25	$1\frac{1}{3}$	23.45	0.2436	172	0.006473
27	25	25	$1\frac{1}{2}$	23.01	0.2436	206	0.011445
43	25	25	1	22.82	0.2436	221	0.013638
$52\frac{1}{2}$	25	25	1	22.53	0.2436	243	0.016855
67	25	25	1	22.19	0.2436	270	0.020804

Table. 10. Experimental data for Run (12)

L_o = 0.84975 cm
c_{lci} = 54.98 mg/liter

kind of sample (hrs)	volume of sample (cm^3)	volume of $K_2Cr_2O_7$ (cm^3)	boiling time (hrs)	volume of $Fe(NH_4)_2(SO_4)_2$ (cm^3)	normality	COD (mg/liter	corrected dimensionless concentration Y_e
blank		25	1	26.06	0.23983		
4	25	25	$1\frac{1}{2}$	25.40	0.23983	50.65	-0.001470
25	25	25	1	24.80	0.23983	96.70	0.014177
$40\frac{1}{2}$	25	25	1	24.70	0.23983	104.37	0.016784
blank		25	1	26.30	0.23764		
48	25	25	$\frac{5}{6}$	24.80	0.23764	114.07	0.020080
blank		25	1	26.33	0.23737		
54	25	25	1	24.79	0.23737	116.98	0.021068
blank		25	1	26.39	0.23683		
66	25	25	$1\frac{1}{5}$	24.70	0.23683	128.08	0.024340

for both experimental Runs (11) and (12), and therefore, for the both cases, equation (15) is

$$\beta \cot\beta + 0.40571 = 0 \qquad (57).$$

The first twenty eigenvalues which satisfy equation (57) are listed in Table 11. The experimental data Y_e's are shown in Tables 9 and 10 for Runs (11) and (12) respectively. Equation (44) can be rewritten as

$$E(D_{pe}) = \sum_{1}^{m} (Y_c(D_{pe}) - Y_e)^2 \qquad (58).$$

To find the effective pseudo-diffusivity of COD such that the sum of square errors might be minimized, a one-dimensional search technique (the Golden Section method) was used. The computer program is listed in Appendix (G), and the computational results are shown in Figure 23 which indicates that the values of D_{pe} for runs (11) and (12) are 4.22×10^{-6} cm^2/sec and 5.77×10^{-6} cm^2/sec, respectively. In those cases, the values of the standard deviation from equation (51) are found to be 3.133×10^{-3} and 2.077×10^{-3} respectively.

The difference between the two independent experimental results can be largely attributed to the fact that the samples used in the two experiments came from two different batches of the cattle manure. It should be noted that the result of calibration of the experimental set-up (with sucrose solution) in term of a single depth correction factor was used in recovering the diffusivity of COD, and no arbitrary and independent determination of this factor was made in the experiments with manure

Table. 11. Eigenvalues from equation (57).

eigenvalues	for Runs (11) and (12)
β_1	1.79333
β_2	4.79675
β_3	7.90527
β_4	11.03233
β_5	14.16581
β_6	17.30218
β_7	20.44019
β_8	23.57915
β_9	26.71871
β_{10}	29.85877
β_{11}	32.99889
β_{12}	36.13949
β_{13}	39.28022
β_{14}	42.42104
β_{15}	45.56200
β_{16}	48.70300
β_{17}	51.84408
β_{18}	54.98519
β_{19}	58.12640
β_{20}	61.26773

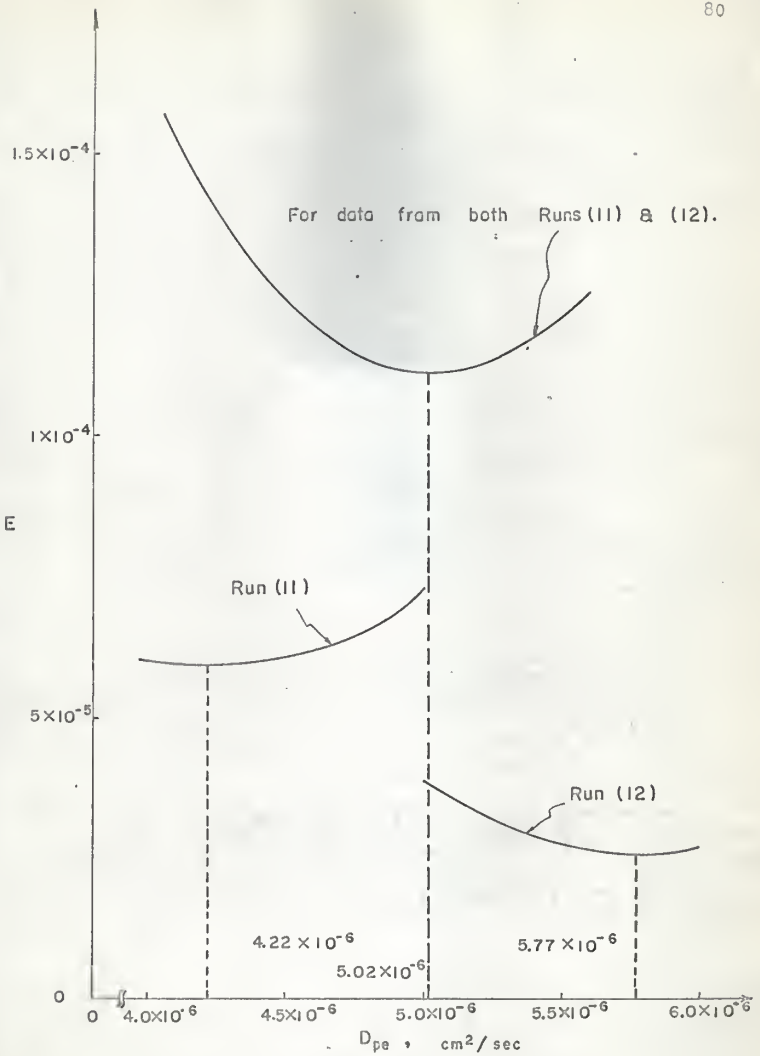

Fig. 23. Effective psuedo-diffusivity of C O D .

solution. This might also give rise to the deviations of the results from two experiments. Of course, the other obvious sources of the error are the assumptions that the complex manure solution is a binary mixture and that the diffusivity is constant. Considering those factors, the agreement between the two sets of results can be said to be very remarkable.

To determine the average value of D_{pe}, all data from both runs were reanalyzed jointly. This value was found to be 5.02×10^{-6} cm²/sec (see Figure 23). The standard deviation was 3.049×10^{-3}.

To estimate the maximum possible error from this average value of D_{pe}, the following effects are considered; that is, temperature, concentration, and correction factor. To estimate the effects of temperature and concentration on the diffusivity of COD, it is assumed that the organic matter in cattle feedlot runoff is sucrose. For an aqueous sucrose solution, the effects of temperature and concentration on the diffusivity are roughly 1.6×10^{-7} cm²/sec °C and 3.5×10^{-7} cm²/sec mole (15). According to the experimental conditions listed in Table 8, the maximum possible temperature and concentration deviations are about 4 °C and 0.5 moles. Thus, the maximum possible errors due to temperature and concentration deviations are approximately 6.4×10^{-7} cm²/sec and 1.75×10^{-7} cm²/sec respectively.

To estimate the possible error due to the correction factor, the correction factor of 1.0037 cm obtained from a single run (Run (3)) was used for the determination of the effective pseudo-diffusivity by using all data instead of the average correction

factor (0.84975 cm). It was found to be 3.59×10^{-6} cm²/sec. This indicates that the possible error due to the correction factor is approximately $5.02 \times 10^{-6} - 3.59 \times 10^{-6} = 1.43 \times 10^{-6}$ (cm²/sec) in the units of effective diffusivity.

The total maximum error can be summed to be $[(6.4 \times 10^{-7} + 1.75 \times 10^{-7})/\sqrt{2}] + 1.43 \times 10^{-6} = 2.01 \times 10^{-6}$ cm²/sec in the units of effective diffusivity. This corresponds to 40% error from the average D_{pe}, 5.02×10^{-6} cm²/sec.

An approximate value of the diffusivity of COD can be roughly estimated as follows: Although the composition of cattle manure depends on their feed ration, it has been shown that its components are roughly 65 — 75% carbohydrates (15 — 20% of crude fiber and 45 — 60% of N-free extract), 15 — 20% protein (N x 6.25), 5 — 15% ash, and 1 — 5% extract ether (21). Thus, in the cattle manure solution, there are carbohydrates, protein, ash and ether. However, most organic materials are carbohydrates and ether is quite rare. According to the International Critical Tables (14) and Gosting (22), the approximate overall diffusivity of carbohydrates is about 6.0×10^{-6} cm²/sec and that of protein is about 1.0×10^{-7} cm²/sec. Therefore, the so-called pseudo-molecular diffusivity of COD in feedlot runoff can be estimated to be about 5.5×10^{-6} cm²/sec. In the units of the effective pseudo-diffusivity, it is approximately 4.0×10^{-6} cm²/sec.

If the experimental and estimated values are compared to each other, the experimental value is slightly larger than the approximate value given above. This can be accounted for by the fact that the manure solutions used in the experiments were not

completely homogeneous even though they had been filtered twice. That is, it is supposed that there was a considerable amount of fine suspensions in the solutions which gave rise to an increase in the experimentally determined value. All experimental results are shown in Figure 24.

CONCLUSIONS

The effective pseudo-diffusivity of COD through a porous stratum (medium) saturated by water was obtained. The average value of the effective pseudo-diffusivity of COD was found to be approximately 5.02×10^{-6} cm^2/sec at a temperature of 25 ± 2 °C. This corresponds to the pseudo-molecular diffusivity of COD in water of 7.10×10^{-6} cm^2/sec.

Information generated in this study is pertinent to water pollution caused by feedlot runoff. Since the effective pseudo-diffusivity of COD through the porous stratum saturated by water is small, it can be said that organic matter which diffuses from the earth underneath the feedlot to the surface of the lot probably does not contribute appreciably to the pollution due to the feedlot runoff.

According to Miner (4), considerable quantities of suspended solids were washed from the feedlot during runoff in his experiments. The conditions of high COD concentration corresponded to the conditions of high concentration of solid suspension. It may be concluded that as far as COD is concerned, the main contribution to the pollution due to the feedlot runoff is the manure suspension moving along with the runoff water.

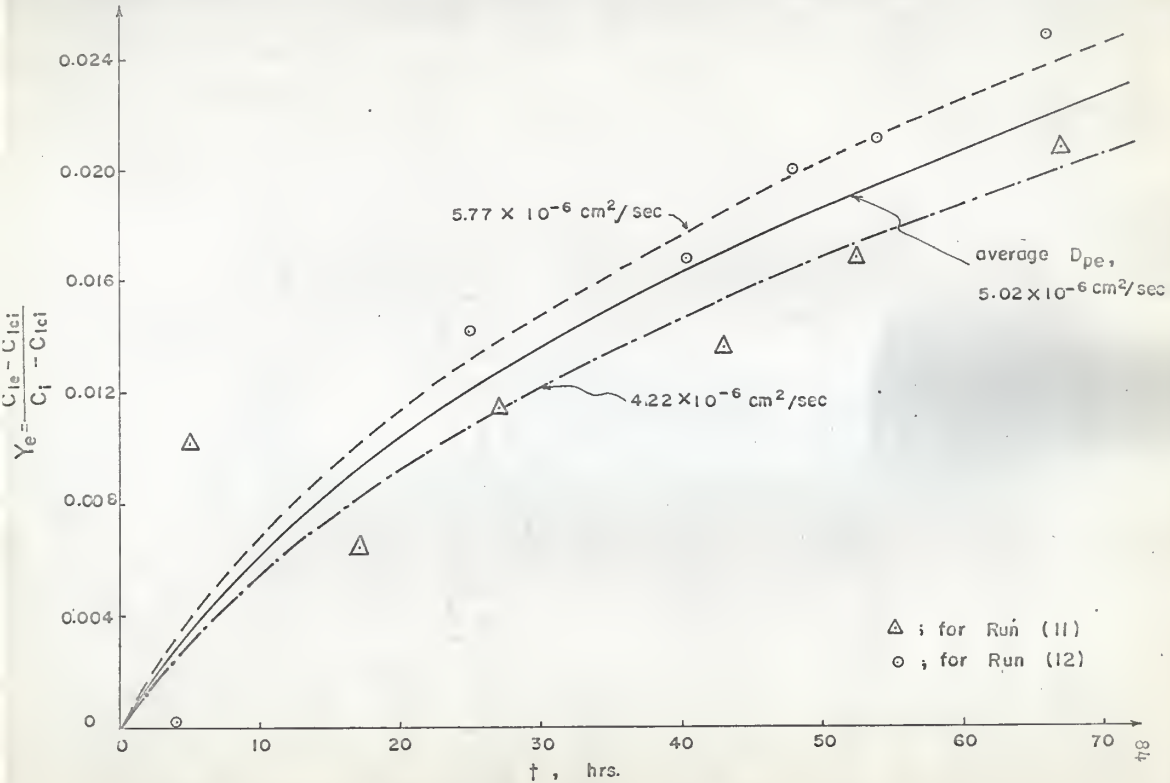

Fig. 24. Plot of experimental data for Runs (11) & (12).

NOMENCLATURE

a	arbitrary constant
A	cross-sectional area, cm^2
b	arbitrary constant
BOD	biochemical oxygen demand, mg/liter
c	concentration of the packed bed based on its void space, g-moles/liter or mg/liter
c_i	initial concentration of the packed bed based on its void space, g-moles/liter or mg/liter
c_1	concentration of the solution in the upper reservoir, g-moles/liter or mg/liter
c_{1ci}	corrected value of c_{1i}, g-moles/liter or mg/liter
c_{1e}	experimental value of c_1, g-moles/liter or mg/liter
c_{1i}	initial concentration of the solution in the upper reservoir, g-moles/liter or mg/liter
COD	chemical oxygen demand, mg/liter
D_e	effective diffusion coefficient through a porous packed bed defined by equations (1), (2) and (3), cm^2/sec
D_o	molecular diffusion coefficient, cm^2/sec
D_p	pseudo-molecular diffusivity of COD which represents the overall true diffusivity of various types of organic matter, cm^2/sec
D_{pe}	effective pseudo-diffusivity of COD through a porous packed bed, cm^2/sec
E	sum of square errors
F	assumed particular solution of $\bar{X}$
k	irreversible first order homogeneous reaction constant, hr^{-1} or sec^{-1}
K	modified effective diffusion coefficient, cm^2/sec
L	thickness of packed bed or arbitrary length, cm
L_c	corrected thickness of packed bed, cm

L_o depth correction factor, cm

m number of data

n number

N normal concentration, No. of equivalents of solute/liter

p(s), p_1(s), q(s), q_1(s) and Q_1(s) functions of Laplace Transformation parameter s

P porosity of the packed bed

R dimensionless reaction constant, kL^2/D_e

R_1 dimensionless reaction constant, $kV^2/D_eP^2A^2$

r_n residue of Laplace transformed functions $\bar{Y}(s)$ and $\bar{X}(s)$

s Laplace transformation parameter

S negative value of dimensionless concentration Y when $c_1 = 0$, $c_{11}/(c_i - c_{11})$

S_i same as S

s_n pole of a function

t time, hr or sec

T tortuosity of the packed bed

u volume of $Fe(NH_4)_2(SO_4)_2$ used for blank, cm^3

v volume of $Fe(NH_4)_2(SO_4)_2$ used for sample, cm^3

V volume of the solution in the upper reservoir, cm^3

V_c corrected value of V, cm^3

w normality of $Fe(NH_4)_2(SO_4)_2$

x weight % concentration of sucrose solution measured by refractometer, wt of sucrose/total wt

X dimensionless concentration within the packed bed, $(c - c_{11})/(c_i - c_{11})$

$\bar{X}$ Laplace transform of X

$\bar{X}_n$ homogeneous solution of $\bar{X}$

$\bar{X}_p$ particular solution of $\bar{X}$

y	real weight % concentration of sucrose solution, wt of sucrose/total wt
Y	dimensionless concentration in the upper reservoir, $(c_1 - c_{11})/(c_i - c_{11})$
Y_c	corrected value of Y
Y_e	corrected experimental value of Y
$\overline{Y}$	Laplace transform of Y
z	distance from the interface in the direction of the packed bed, cm
Δz	differential value of z, cm

Greek Symbols

α	dimensionless constant, ALP/V
β_n	eigenvalue which satisfies equation (15)
θ	dimensionless time, $D_e t/L^2$
θ_1	dimensionless time, $D_e A^2 P^2 t/V^2$
λ	dimensionless distance, z/L
λ_1	dimensionless distance, APz/V
π	effect of agitating motor expressed in diffusivity unit, cm^2/sec
σ	standard deviation
Σ	summation operator sign

ACKNOWLEDGMENTS

The author wishes to offer his sincere thanks and grateful appreciations to his major advisor, Dr. Liang-tseng Fan, and to Dr. Larry E. Erickson for their constant advice and guidance in this study. The author also expresses his gratitude to Professor Ralph I. Lipper, for his helpful suggestions and reading of the manuscript. Dr. Richard G. Akins should also be acknowleged for his help in reading the manuscript. And finally, the author sends his thanks to the Agricultural Experiment Station at Kansas State University for financially supporting this work (Project No.0660).

BIBLIOGRAPHY

1. Henderson, J. M., "Agricultural Land Drainage and Stream Pollution" J. of San. Eng. Div., ASCE., 88, SA 6, 61-(1962)

2. Smith, S.M. and Miner, J. R., "Stream Pollution from Feedlot Runoff" Proc. 14th San. Eng. Conf., University of Kansas, Lawrence, Kan. (1964)

3. Miner, J. R., Fina, L. R., Funk, J. W., Lipper, R. I. and Larson, G. H., "Stormwater Runoff from Cattle Feedlot" JWPCF., 38, 10, (October 1966)

4. Miner. J. R., "Water Pollution Potential of Cattle Feedlot Runoff" Ph. D. Dissertation, Kansas State University (1967)

5. Sawyer, C. N., "Chemistry for Sanitary Engineers" McGraw-Hill Inc. (1960)

6. Mckinney, R. E., "Microbiology for Sanitary Engineers." McGraw-Hill Inc. (1962)

7. Crank, J., "The Mathematics of Diffusion" Oxford University Press, London, (1956)

8. Crank, J., "A Diffusion Problem in which the Amount of Diffusing Substance is Finite — Diffusion with Non-Linear Adsorption." Phil. Mag., 39, 140 (1948)

9. Danckwerts, P. V., "Absorption by Simultaneous Diffusion and Chemical Reaction into Particles of Various Shapes and into falling Drops" Trans. Faraday Soc., 47, 1014-1023 (1951)

10. Wilson, A. H., "A Diffusion Problem in which the Amount of Diffusing Substance is Finite" Phil. Mag., 39, 48 (1948)

11. Erdelyi, A., Magnus, W., Oberhettinger, F. and Tricomi, F. G., "Table of Intergral Transforms" Vol. I, Bateman Manuscript Project, McGraw-Hill Inc. (1954)

12. Churchill, R. V., "Operational Mathematics" second edition, McGraw-Hill Inc., (1958)

13. Brid, R. B., Stewart, W. E. and Lightfoot, E. N., "Transport Phenomena" John Wiley & Sons Inc. (1960)

14. National Research Council, "International Critical Tables of Numerical Data Physics, Chemistry and Technology" McGraw-Hill Inc. (1926-1933)

15. Henrion, P. N., "Diffusion in the Sucrose + Water System"

Trans. Faraday Soc., 60(1), 72-74 (1964)

16. Van Hook, A. and Russell, H. D., "The diffusivities of Concentrated Sucrose Solutions" J. Am. Chem. Soc., 67, 370 (1945)

17. Penman, H. L., "Gas and Vapour Movements in the Soil" J. of Agri. Science., 30, 437 and 570 (1940)

18. Carman P. C., "Flow of Gases Through Porous Media", Butterworths Scientific Publications, London (1956)

19. Bausch & Lomb Incorporated, "Baush & Lomb Refractometer Reference Manual" 2nd. Ed., New York.

20. American Public Health Association, "Standard Methods for the Examination of Water and Wastewater", 11st. Ed., New York (1960).

21. Drake, C. L., Unpublished Experimental Data, Department of Animal Husbandry, Kansas State University.

22. Gosting, L. J., "Measurement and Interpretation of Diffusion Coefficients of Proteins", Advances in Protein Chemistry, Vol. XI, Academic Press Inc., New York (1956).

23. Hogg, R. V. and Craig, A. T. "Introduction to Mathematical Statistics" second edition Macmillan Co. (1965)

24. Chen, G. K. C., "Modeling and Optimization of the Hydraulic Regime of Activated Sludge Systems" M.S. Thesis, Kansas State University (1968)

APPENDIX. A.

SHELL MASS BALANCE IN POROUS MEDIA.

A shell mass balance is made over an arbitrary differential bed element to establish the differential equation for the diffusional process taking place in the system of a binary fluid mixture of species B and W in a packed bed. The law of conservation of mass of species B is applied to a volume element of the packed bed $\Delta z A$ fixed in the system shown in Figure A-1, in which a binary mixture of B and W is placed. For this packed bed system, a shell mass balance can be made in two ways. In the first approach, the packed bed is assumed as a homogeneous liquid layer and a shell mass balance is obtained by using a modified molecular diffusion coefficient, the effective diffusion coefficient, in place of the molecular diffusion coefficient. In the second approach, the system is considered to be composed of two parts, the continuous solid phase and the continuous liquid phase which exist parallel in the vertical direction. Mass transfer occurs only in the continuous liquid phase by the molecular diffusion.

The final resulting diffusion equations from these two different approaches should be interrelated. This implies that there exists a relation between the effective diffusion coefficient and the molecular diffusion coefficient. Here, it is assumed that the porous packed bed is isotropic, i.e., the pore space is randomly distributed and in any cross-sectional area the fraction not occupied by solids is always the same.

METHOD I

In the first approach, the packed bed of the system shown in Figure A-1 is assumed as a homogeneous liquid layer. The

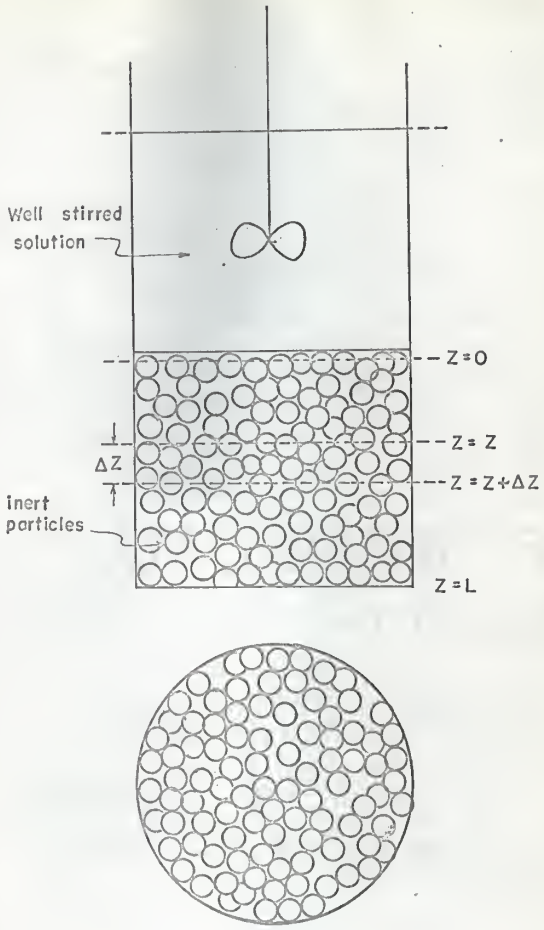

Fig. A-1. Schematic diagram of the experimental set-up comprised of a packed bed & a well stirred solution.

concentration of the homogeneous layer is defined as the moles of species B which exist in the void space of the packed bed divided by the total volume of the bed. A shell mass balance is made within the hypothetical homogeneous layer as follows:

molar accumulation rate of B the volume element of the bed	$\frac{\partial c_b}{\partial t}$ (AzA)
input of B across the cross-sectional area	$N_B\big\|_{z+\Delta z}$ A
output of B across the cross-sectional area	$N_B\big\|_{z}$ A.

When the entire mass balance is written and divided through by AzA,

$$\frac{\partial c_b}{\partial t} = \frac{\partial N_B}{\partial z} \qquad \text{(A-1)}$$

is obtained by letting the size of the distance element decrease to zero. In this case, the molar flux of species B, N_B, is expressed by using an effective diffusion coefficient D_e in place of the molecular diffusion coefficient D_o. The molar flux is written as

$$N_B = D_e \frac{\partial c_b}{\partial z} \qquad \text{(A-2).}$$

By substituting equation (A-2) into equation (A-1)

$$\frac{\partial c_b}{\partial t} = D_e \frac{\partial^2 c_b}{\partial z^2} \qquad \text{(A-3)}$$

is obtained.

Another shell mass balance is made at the interface of the

upper solution and the hypothetical homogeneous liquid layer as follows:

molar accumulation rate of B in the volume of upper layer	$\frac{dc_1}{dt} V_1$
input of B across the cross-sectional area	$N_B\big\|_{z=0} A$
output of B across the cross-sectional area	0.

When the entire mass balance is written

$$V_1 \frac{dc_1}{dt} = N_B\Big|_{z=0} A \tag{A-4}$$

or

$$V_1 \frac{dc_1}{dt} = D_e \frac{\partial c_b}{\partial z}\Big|_{z=0} A \tag{A-5}$$

is obtained.

The initial and boundary conditions can also be established as follows:

(1) The concentrations within the hypothetical homogeneous layer and the upper reservoir are initially c_{bi} and c_{li} throughout; that is, when $t = 0$,

$$c_b = c_{bi}$$

$$c_l = c_{li}.$$

(2) At the interface of the two layers, the concentrations of both layers have the relationship; that is, at $z = 0$,

$$c_b = Pc_l \quad \text{for } t > 0.$$

(3) There is no mass transfer at the bottom of the lower layer; that is, at $z = L$

$$\frac{\partial c_b}{\partial z} = 0.$$

Nomenclature

A = total cross-sectional area, cm^2

c_b = bulk concentration of species B within the hypothetical homogeneous layer, that is, the moles of species B within the void space of the bed divided by the total volume, g-moles/cm^3

c_1 = concentration of species B in the upper reservoir, g-moles/cm^3

D_e = effective diffusion coefficient of species B, cm^2/sec

D_o = molecular diffusion coefficient of species B, cm^2/sec

N_B = molar flux of species B based on the bulk concentration of the homogeneous layer, g-moles/cm^2sec

P = porosity of the bed

t = time, sec

V_1 = volume of the upper solution, cm^3

z = distance from the interface of the two layers in the direction of the bottom, cm

METHOD II

The second approach visualizes the system as shown in Figure A-2. A shell mass balance is made within the lower bed of the system shown in Figure A-2 as follows:

molar accumulation of B in volume element of the bed	$\frac{\partial c}{\partial t}(\Delta z PA)$
input of B across the reduced area of cross-section available for molecular movements	$N_B\Big\|_{z+\Delta z}(PA)$

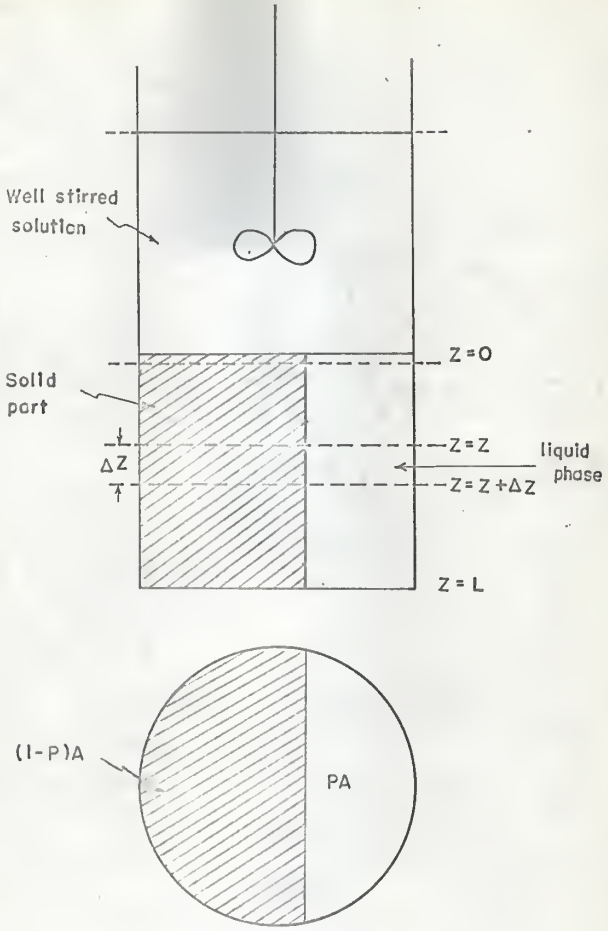

Fig. A-2. Schematic diagram of the system equivalent to that shown in Fig.A-1 .

output of B across the reduced area of cross-section available for molecular movements	$N_B\big\|_z$ (PA)

If the entire mass balance is written and divided through by $\Delta z PA$,

$$\frac{\partial c}{\partial t} = \frac{\partial N_B}{\partial z} \qquad \text{(A-6)}$$

is obtained by letting the size of the distance element decrease to zero. Since there is no bulk flow in the system, the molar flux is written as

$$N_B = D_o \frac{\partial c}{\partial z} \qquad \text{(A-7)}.$$

According to Penman (17) and Carman (18), the rate of diffusion through a porous body is reduced due to the increased path length imposed by the tortuous nature of the channels which the molecular current must follow. Thus, the actual molar flux through the original packed is smaller than that through the system shown in Figure A-2 by a factor of $\frac{1}{T}$. T is the tortuosity of the bed — i.e., the ratio of the path length through the porous medium to the direct or "crow-flight" distance through the medium. The tortuosity is always larger than unity. The actual molar flux $(N_B)_a$ can be written as

$$(N_B)_a = \frac{N_B}{T} \qquad \text{(A-8)}$$

and must be used in place of N_B in equation (A-6). Equation (A-6) is rewritten as

$$\frac{\partial c}{\partial t} = \frac{\partial (N_B)_a}{\partial z}$$

or

$$\frac{\partial c}{\partial t} = \frac{1}{T}\frac{\partial N_B}{\partial z}$$

$$= \frac{D_o}{T}\frac{\partial^2 c}{\partial z^2} \qquad \text{(A-9).}$$

Also, if another shell mass balance is obtained at the interface of the two layers,

$$V_L \frac{dc_1}{dt} = \frac{D_o}{T}\frac{\partial c}{\partial z}\bigg|_{z=0} \text{ (PA)} \qquad \text{(A-10)}$$

is obtained.

The initial and boundary conditions are as follows:

(1) When $t = 0$,

$c = c_i$

$c_1 = c_{1i}$.

(2) At $z = 0$,

$c = c_1$ for $t > 0$.

(3) At $z = L$,

$\frac{\partial c}{\partial z} = 0$.

Nomenclature

A = total cross-sectional area of the bed, cm^2

c = concentration of species B in the void space of the bed, that is, the actual concentration of the fluid within the void space of the bed, g-moles/cm^3

c_L = concentration of species B in the upper reservoir, g-moles/cm^3

D_o = molecular diffusion coefficient of species B, cm^2/sec

$(N_B)a$ = actual molar flux of species B through the porous medium, g-moles/cm^{2}sec

P = porosity of the bed

t = time, sec

T = tortuosity of the bed

V_L = volume of the upper solution, cm^3

z = distance from the interface of the two layers in the direction of the bottom, cm

COMPARISON OF THE TWO METHODS

It can be seen that equation (A-3) corresponds to equation (A-9) and that equation (A-5) corresponds to equation (A-10). In the four equations above, it is obvious that

$$c_b = P\, c,$$

$$c_1 = c_L$$

and

$$V_1 = V_L$$

Therefore, the relation between the effective diffusion coefficient D_e and the molecular diffusion coefficient D_o can be obtained as

$$D_e = \frac{D_o}{T} \qquad \text{(A-11)}.$$

APPENDIX. B.

DERIVATION OF EQUATIONS (22) AND (23) FROM EQUATIONS (20) AND (21) WITH BOUNDARY CONDITIONS.

Equations (20) and (21) are repeated below:

$$\frac{d^2\overline{X}}{d\lambda^2} - (s + R)\,\overline{X} + 1 - \frac{RS}{s} = 0 \qquad (20)$$

$$(s + R)\overline{Y} + \frac{RS}{s} = \alpha \left.\frac{d\overline{X}}{d\lambda}\right|_{\lambda=0} \qquad (21).$$

Boundary conditions are

(i) at $\lambda = 0$, $\overline{X} = \overline{Y}$ for $\theta > 0$ and

(ii) at $\lambda = 1$, $\frac{d\overline{X}}{d\lambda} = 0$.

Equation (20) is a simple ordinary second order differential equation with two boundary conditions. The homogeneous solution, $\overline{X}_h$, for equation (20) can be obtained as

$$\overline{X}_h = a \exp(-\lambda\sqrt{s+R}) + b \exp(\lambda\sqrt{s+R}) \qquad (B\text{-}1)$$

where a and b are arbitrary constants to be determined.

F is assumed to be the particular solution, $\overline{X}_p$, for equation (20); that is,

$$\overline{X}_p = F \qquad (B\text{-}2).$$

Thus, the general solution of equation (20) is

$$\overline{X} = \overline{X}_h + \overline{X}_p = a \exp(-\lambda\sqrt{s+R}) + b \exp(\lambda\sqrt{s+R}) + F \qquad (B\text{-}3).$$

In order to evaluate F, equation (B-3) is substituted into equation (20) and equation (B-4) is obtained as follows:

$$\frac{d^2\overline{X}}{d\lambda^2} - (s + R)\overline{X} + 1 - \frac{RS}{s}$$

$$= (s + R)\left[a \exp(-\lambda\sqrt{s+R}) + b \exp(\lambda\sqrt{s+R})\right]$$
$$- (s + R)\left[a \exp(-\lambda\sqrt{s+R}) + b \exp(\lambda\sqrt{s+R}) + F\right] + 1 - \frac{RS}{s} = 0$$

or $$F = \frac{s - RS}{s(s + R)} \qquad \text{(B-4)}.$$

Substituting equation (B-4) into equation (B-3), equation (B-3) becomes

$$\overline{X} = a \exp(-\lambda\sqrt{s+R}) + b \exp(\lambda\sqrt{s+R}) + \frac{s - RS}{s(s + R)} \qquad \text{(B-5)}.$$

Now the integral constants a and b must be determined with boundary conditions (i) and (ii). From boundary condition (i),

$$Y = a + b + \frac{s - RS}{s(s + R)} \qquad \text{(B-6)}.$$

From boundary condition (ii),

$$\left.\frac{d\overline{X}}{d\lambda}\right|_{\lambda=1} = \sqrt{s+R}\left[b \exp(\sqrt{s+R}) - a \exp(-\sqrt{s+R})\right] = 0$$

or $$a = b \exp(2\sqrt{s+R}) \qquad \text{(B-7)}.$$

If equations (B-6) and (B-7) are solved simultaneously with respect to a and b, the following equations are obtained.

$$a = \frac{\exp(2\sqrt{s+R})\left[\overline{Y} - \frac{s - RS}{s(s + R)}\right]}{1 + \exp(2\sqrt{s+R})} \qquad \text{(B-8)}$$

and

$$b = \frac{\overline{Y} - \frac{s - RS}{s(s + R)}}{1 + \exp(2\sqrt{s+R})} \qquad \text{(B-9)}.$$

Substituting equations (B-8) and (B-9) into equation (B-5),

it yields

$$\bar{X} = \left[\frac{\bar{Y} - \frac{s - RS}{s(s + R)}}{1 + \exp(2\sqrt{s+R})}\right]\left[\exp((2 - \lambda)\sqrt{s+R}) + \exp(\lambda\sqrt{s+R})\right]$$

$$+ \frac{s - RS}{s(s + R)} \qquad (22).$$

By substitution of equation (22) into equation (21), $\bar{Y}$ can be obtained as follows:

$$\bar{Y} = \frac{\alpha\ (\exp(2\sqrt{s+R}) - 1)}{(s + R)\left[\sqrt{s+R}(\exp 2(\sqrt{s+R}) + 1) + \alpha\ (\exp(2\sqrt{s+R}) - 1)\right]}$$

$$- \frac{RS}{s(s + R)} \qquad (23).$$

APPENDIX. C.

DERIVATION OF EQUATIONS (28) AND (29) FROM EQUATIONS (26) AND (27).

Equation (26) is repeated below:

$$\bar{Y} = \frac{\alpha \sinh(\sqrt{s+R})}{(s+R)[\sqrt{s+R}\cosh(\sqrt{s+R}) + \alpha \sinh(\sqrt{s+R})]} - \frac{RS}{s(s+R)}$$

$$= \bar{Y}_1 - \bar{Y}_2 \qquad (26)$$

where

$$\bar{Y}_1 = \frac{\alpha \sinh(\sqrt{s+R})}{(s+R)[\sqrt{s+R}\cosh(\sqrt{s+R}) + \alpha \sinh(\sqrt{s+R})]} \qquad (C\text{-}1)$$

and

$$\bar{Y}_2 = \frac{RS}{s(s+R)} \qquad (C\text{-}2).$$

In order to obtain the inverse Laplace transforms of $\bar{Y}_1$ and $\bar{Y}_2$, the residue theory (12) can be used. According to the residue theory (12), the inverse transform of $\bar{Y}$ is represented as the series of residue of $\exp(s\theta)\ \bar{Y}$:

$$Y(\theta) = \sum_{n=1}^{\infty} r_n(\theta) \qquad (C\text{-}3).$$

When a pole s_n is a simple pole, the residue can be written as

$$r_n(\theta) = \lim_{s \to s_n} (s - s_n) \exp(s\theta)\ \bar{Y}(s)$$

$$= \exp(s_n\theta) \lim_{s \to s_n} (s - s_n)\ \bar{Y}(s) \qquad (C\text{-}4).$$

If, in a particular case, in which $\bar{Y}(s)$ has a fractional form, such as

$$\bar{Y}(s) = \frac{p(s)}{q(s)} \qquad (C\text{-}5),$$

Where $p(s)$ and $q(s)$ are analytic at $s = s_n$ and $p(s_n) \neq 0$, then

the residue can be expressed as

$$r_n(\theta) = \frac{p(s_n)}{q'(s_n)} \exp(s_n\theta) \qquad \text{(C-6)}.$$

Therefore, equation (C-3) becomes

$$Y(\theta) = \sum_{n=1}^{\infty} \frac{p(s_n)}{q'(s_n)} \exp(s_n\theta) \qquad \text{(C-7)}.$$

First, the inverse form of $\bar{Y}_1$ is obtained. Poles of equation (C-1) are where

$$s + R = 0 \qquad \text{(C-8)}.$$

$$\sqrt{s+R}\cosh(\sqrt{s+R}) + \alpha \sinh(\sqrt{s+R}) = 0 \qquad \text{(C-9)}.$$

It is obvious that the pole from equation (C-8) is simple, and that from equation (C-9) an infinite number of poles are obtained.

From equation (C-1),

$$\bar{Y}_1 = \frac{p_1(s)}{q_1(s)} = \frac{p_1(s)}{(s+R)\,Q_1(s)} \qquad \text{(C-10)}$$

where,

$$p_1(s) = \alpha \sinh(\sqrt{s+R})$$

$$q_1(s) = (s+R)\left[\sqrt{s+R}\cosh(\sqrt{s+R}) + \alpha \sinh(\sqrt{s+R})\right]$$

$$Q_1(s) = \sqrt{s+R}\cosh(\sqrt{s+R}) + \alpha \sinh(\sqrt{s+R}).$$

From equation (C-8),

$$s_n = -R \qquad \text{(C-11)}.$$

Since $p_1(-R) = 0$, L'Hospital's Rule must be used to obtain the

residue. Then,

$$r(\theta) = \exp(-R\theta) \lim_{s \to -R} \frac{p_1'(s)}{q_1'(s)} = \left(\frac{\alpha}{1+\alpha}\right) \exp(-R\theta) \qquad (C\text{-}12).$$

From equation (C-9), it can be shown that $\sqrt{s+R}$ is a pure imaginary number; that is,

$$\sqrt{s_n+R} = i\,\beta_n$$

or
$$s_n = -(\beta_n^2 + R) \qquad (C\text{-}13).$$

Thus, equation (C-9) can be rewritten as follows:

$$\sqrt{s+R}\cosh(\sqrt{s+R}) + \alpha \sinh(\sqrt{s+R}) = i\,\beta\cos\beta + i\,\alpha\sin\beta = 0$$

or
$$\beta\cot\beta + \alpha = 0 \qquad (C\text{-}14).$$

Now, an infinite number of β, i.e., β_1, β_2, ..., β_n ...., which satisfy equation (C-14) can be obtained. Accordingly, an infinite number of poles, i.e., s_1, s_2, ..., s_n ....., which satify equation (C-9) can be calculated. By the residue theory,

$$r_n(\theta) = \lim_{s \to s_n} \frac{p_1(s)}{q_1'(s)} \exp(s\theta)$$

$$= \frac{\alpha \sinh(\sqrt{s_n+R}) \exp(s_n\theta)}{(s_n+R)\left[\frac{1}{2\sqrt{s_n+R}}\cosh(\sqrt{s_n+R}) + \frac{1}{2}\sinh(\sqrt{s_n+R}) + \frac{\alpha}{2\sqrt{s_n+R}}\cosh(\sqrt{s_n+R})\right]} \qquad (C\text{-}15).$$

Since,

$$\sinh(\sqrt{s_n+R}) = -\frac{\sqrt{s_n+R}}{\alpha}\cosh(\sqrt{s_n+R})$$

and

$$s_n = -(\beta_n^2 + R),$$

$$r_n(\theta) = -\frac{2}{1 + \alpha + \frac{\beta_n^2}{\alpha}} \exp(-(\beta_n^2 + R)\theta) \qquad \text{(C-16)}.$$

Here, an infinite number of $r_n(\theta)$ are obtained.

From equations (C-12) and (C-16), the inverse transform of $\bar{Y}_1(s)$, $Y_1(\theta)$, is produced as follows:

$$Y_1(\theta) = \left(\frac{\alpha}{1 + \alpha}\right) \exp(-R\theta) - \sum_{n=1}^{\infty} \frac{2 \exp(-(\beta_n^2 + R)\theta)}{\left(1 + \alpha + \frac{\beta_n^2}{\alpha}\right)} \qquad \text{(C-17)}.$$

Next, the inverse form of $\bar{Y}_2$ is obtained. In equation (C-2), there exist two poles given in the the following equations:

$$s = 0 \qquad \text{(C-18)},$$

$$s + R = 0 \qquad \text{(C-19)}.$$

Similarly,

$$r_n(\theta) = \lim_{s \to 0} s\, \bar{Y}_2(s) = S \qquad \text{(C-20)}$$

for $s = 0$, and

$$r_n(\theta) = \lim_{s \to -R} (s + R)\, \bar{Y}_2(s) \exp(s\theta)$$

$$= -S \exp(-R\theta) \qquad \text{(C-21)}$$

for $s = -R$.

Therefore, from equations (C-20) and (C-21) the inverse transform of $\bar{Y}_2(s)$, $Y_2(\theta)$, can be obtained as follows:

$$Y_2(\theta) = S(1 - \exp(-R\theta)) \qquad \text{(C-22)}.$$

Finally, the inverse transform of $\bar{Y}(s)$, $Y(\theta)$, can be derived as follows:

$$Y(\theta) = Y_1(\theta) - Y_2(\theta)$$

$$= \frac{\alpha}{1+\alpha}\exp(-R\theta) - \sum_{n=1}^{\infty} \frac{2\exp(-(\beta_n^2+R)\theta)}{(1+\alpha+\frac{\beta_n^2}{\alpha})} - S(1-\exp(-R\theta)) \qquad (28).$$

In like manner, equation (27) is repeated as

$$\bar{X} = \frac{\bar{Y} - \frac{s-RS}{s(s+R)}}{1+\exp(2\sqrt{s+R})}\left[\exp((2-\lambda)\sqrt{s+R}) + \exp(\lambda\sqrt{s+R})\right] + \frac{s-RS}{s(s+R)}$$

$$= \bar{X}_1 - \bar{X}_2 - \bar{X}_3 \qquad (27),$$

where,

$$\bar{X}_1 = \frac{1}{s+R} \qquad \text{(C-23)},$$

$$\bar{X}_2 = \frac{\sqrt{s+R}\cosh(\sqrt{s+R}(1-\lambda))}{(s+R)[\sqrt{s+R}\cosh(\sqrt{s+R}) + \alpha\sinh(\sqrt{s+R})]} \qquad \text{(C-24)},$$

$$\bar{X}_3 = \frac{RS}{s(s+R)} \qquad \text{(C-25)}.$$

The inverse transform of $\bar{X}$ can be expressed by inverse transforms of $\bar{X}_1$, $\bar{X}_2$ and $\bar{X}_3$. Then, the inverse transforms of $\bar{X}_1$, $\bar{X}_2$ and X_3, i.e., $X_1(\theta,\lambda)$, $X_2(\theta,\lambda)$ and $X_3(\theta,\lambda)$ can be obtained by the same method used before. Finally, the following equations are derived:

$$X_1(\theta,\lambda) = \exp(-R\theta) \qquad \text{(C-26)}.$$

$$X_2(\theta,\lambda) = \frac{1}{1+\alpha}\exp(-R\theta) + \sum_{n=1}^{\infty} \frac{2\cos(\beta_n(1-\lambda))}{(1+\alpha+\frac{\beta_n^2}{\alpha})\cos\beta_n}\exp(-(\beta_n^2+R)\theta)$$

(C-27).

$$X_3(\theta,\lambda) = S(1 - \exp(-R\theta)) \qquad \text{(C-28)}.$$

Thus, by the substitution of equations (C-26), (C-27) and (C-28) into equation (27)

$$X(\theta,\lambda) = X_1(\theta,\lambda) - X_2(\theta,\lambda) - X_3(\theta,\lambda)$$

$$= \frac{\alpha}{1+\alpha}\exp(-R\theta) - \sum_{n=1}^{\infty} \frac{2\cos(\beta_n(1-\lambda))}{(1+\alpha+\frac{\beta_n^2}{\alpha})\cos\beta_n}\exp(-(\beta_n^2+R)\theta)$$

$$- S(1 - \exp(-R\theta)) \qquad (29).$$

APPENDIX. D.

DERIVATION OF EQUATIONS (35) AND (36) FROM EQUATIONS (33) AND (34).

Equations (33) and (34) are repeated below:

$$\frac{d^2\overline{X}}{d\lambda_1^2} - s\overline{X} + 1 = 0 \qquad (33),$$

$$\overline{Y} = \frac{1}{s}\left.\frac{d\overline{X}}{d\lambda_1}\right|_{\lambda_1=0} \qquad (34).$$

Boundary conditions are

(1) at $\lambda_1 = 0$, $\quad \overline{X} = \overline{Y}$

(2) at $\lambda_1 = \infty$, $\quad \overline{X} = \frac{1}{s}$.

The homogeneous solution for equation (33) can be obtained as

$$\overline{X}_h = a \exp(-\lambda_1\sqrt{s}) + b \exp(\lambda_1\sqrt{s}) \qquad (D\text{-}1),$$

where a and b integral constants to be determined.

If the particular solution for equation (33) is assumed to be F, then the general solution is expressed as

$$\overline{X} = a \exp(-\lambda_1\sqrt{s}) + b \exp(\lambda_1\sqrt{s}) + F \qquad (D\text{-}2).$$

In order to evaluate F, equation (D-2) is substituted into equation (33), and equation (D-3) is obtained as follows:

$$\frac{d^2\overline{X}}{d\lambda_1^2} - s\overline{X} + 1 = s\left[a \exp(-\lambda_1\sqrt{s}) + b \exp(\lambda_1\sqrt{s})\right] - s\left[a \exp(-\lambda_1\sqrt{s}) + b \exp(\lambda_1\sqrt{s}) + F\right] + 1 = 0$$

or $$F = \frac{1}{s} \qquad (D\text{-}3).$$

By substituting equation (D-3) into equation (D-2), equation (D-4) is produced as follows:

$$\overline{X} = a \exp(-\lambda_i \sqrt{s}) + b \exp(\lambda_i \sqrt{s}) + \frac{1}{s} \qquad (D\text{-}4).$$

Now the integral constants a and b must be determined with two boundary conditions. Boundary condition (1) implies that

$$\overline{Y} = a + b + \frac{1}{s} \qquad (D\text{-}5).$$

Also, boundary condition (2) implies that

$$b = 0 \qquad (D\text{-}6).$$

Thus,

$$a = \overline{Y} - \frac{1}{s} \qquad (D\text{-}7).$$

By substituing equations (D-6) and (D-7) into equation (D-4), equation (35) is obtained:

$$\overline{X} = (\overline{Y} - \frac{1}{s}) \exp(-\lambda_i \sqrt{s}) + \frac{1}{s} \qquad (35).$$

Now the expression for $\overline{Y}$ is found by substituting equation (35) into equation (34). That is,

$$\overline{Y} = \frac{1}{s} \frac{d\overline{X}}{d\lambda_i}\bigg|_{\lambda_i=0}$$

$$= -\frac{\overline{Y}}{\sqrt{s}} + \frac{1}{s\sqrt{s}}$$

or $$\overline{Y} = \frac{1}{s(1+\sqrt{s})} \qquad (36).$$

APPENDIX. E.

DERIVATION OF EQUATIONS (41) AND (42) FROM EQUATIONS (39) AND (40).

Here, analytical solutions for equations (39) and (40) are derived with three initial and boundary conditions. These equations are

$$\frac{\partial X}{\partial \theta_1} = \frac{\partial^2 X}{\partial \lambda_1^2} - R_1(X + S_1) \tag{39}$$

$$\frac{dY}{d\theta_1} + R_1(Y + S_1) = \frac{\partial X}{\partial \lambda_1}\bigg|_{\lambda_1=0} \tag{40}$$

with initial and boundary conditions,

(1) when $\theta_1 = 0$,

$$X = 1$$

and

$$Y = 0,$$

(2) at $\lambda_1 = 0$,

$$X = Y \quad \text{for } \theta_1 > 0,$$

and

(3) at $\lambda_1 = \infty$,

$$\frac{dX}{d\theta_1} = -R_1(X + S_1).$$

By making Laplace transforms of equations (39) and (40), and the initial and boundary conditions with respect to θ_1,

$$\frac{d^2\overline{X}}{d\lambda_1^2} - (s + R_1)\overline{X} + 1 - \frac{R_1 S_1}{s} = 0 \tag{E-1},$$

$$(s + R_1)\overline{Y} + \frac{R_1 S_1}{s} = \frac{d\overline{X}}{d\lambda_1}\bigg|_{\lambda_1=0} \tag{E-2}$$

and transformed boundary conditions,

(1) at $\lambda_1 = 0$, $\quad \overline{X} = \overline{Y}$

(2) at $\lambda_1 = \infty$, $\quad \overline{X} = \dfrac{s - R_1 S_1}{s(s + R_1)}$

are obtained.

With the same method used in Case (III), one can get the general solution for equation (E-1) as follows:

$$\overline{X} = a \exp(-\lambda_1\sqrt{s+R_1}) + b \exp(\lambda_1\sqrt{s+R_1}) + \frac{s - R_1 S_1}{s(s+R_1)} \qquad \text{(E-3)}.$$

Now arbitrary constants a and b are determined with the two boundary conditions above. Boundary condition (1) implies that

$$\overline{Y} = a + b + \frac{s - R_1 S_1}{s(s+R_1)} \qquad \text{(E-4)}.$$

Boundary condition (2) implies that

$$b = 0 \qquad \text{(E-5)}.$$

Thus, $$a = \overline{Y} - \frac{s - R_1 S_1}{s(s+R_1)} \qquad \text{(E-6)}.$$

By substituting equations (E-5) and (E-6) into equation (E-3),

$$\overline{X} = \left(\overline{Y} - \frac{s - R_1 S_1}{s(s+R_1)}\right) \exp(-\lambda_1\sqrt{s+R_1}) + \frac{s - R_1 S_1}{s(s+R_1)} \qquad \text{(E-7)}$$

is obtained.

Now the expression for $\overline{Y}$ is found by the substitution of equation (E-7) into equation (E-2) as follows:

$$(s + R_1)\overline{Y} + \frac{R_1 S_1}{s} = \left.\frac{d\overline{X}}{d\lambda_1}\right|_{\lambda_1=0}$$

$$= (-\sqrt{s+R_1})\left(\overline{Y} - \frac{s - R_1 S_1}{s(s+R_1)}\right)$$

or $$\bar{Y} = \frac{1}{(s+R_i)(\sqrt{s+R_i}+1)} - \frac{R_i S_i}{s(s+R_i)} \qquad (E\text{-}8).$$

The inverse Laplace transform of $\bar{Y}$, $Y(\theta_i)$, can be obtained by using the Table of Inverse Laplace Transformation (11) as follows:

$$Y(\theta_i) = \exp(-R_i\theta_i) - \exp((1-R_i)\theta_i)\ \mathrm{erfc}(\sqrt{\theta_i}) - S_i(1 - \exp(-R_i\theta_i)) \qquad (41).$$

By substituting equation (E-8) into equation (E-7), the following equation is obtained.

$$X = \frac{1}{s+R_i} - \frac{\exp(-\lambda_i\sqrt{s+R_i})}{\sqrt{s+R_i}\ (\sqrt{s+R_i}+1)} - \frac{R_i S_i}{s(s+R_i)} \qquad (E\text{-}9).$$

Also, the inverse form of $\bar{X}$, $X(\theta_i, \lambda_i)$, can be found as

$$X(\theta_i,\lambda_i) = \exp(-R_i\theta_i) - \exp(\lambda_i + (1-R_i)\theta_i)\ \mathrm{erfc}\left(\sqrt{\theta_i}+\frac{\lambda_i}{2\sqrt{\theta_i}}\right) - S_i(1 - \exp(-R_i\theta_i)) \qquad (42).$$

APPENDIX F.

DERIVATION OF THE ANALYTICAL SOLUTION FOR CASE (11) BY USING DIMENSIONLESS GROUP, EQUATION (10.a).

In Case (II), equations (4) and (5) are repeated as

$$\frac{\partial c}{\partial t} = D_e \frac{\partial^2 c}{\partial z^2} - kc \qquad (4),$$

$$V \frac{dc_1}{dt} = D_e \frac{\partial c}{\partial z}\bigg|_{z=0} Pa - Vkc_1 \qquad (5).$$

The initial and boundary conditions are

(1) When $t = 0$,

$$c = c_i$$

and

$$c_1 = c_{1i},$$

(2) at $z = 0$,

$$c = c_1 \quad \text{for } t > 0,$$

and

(3) at $z = L$,

$$\frac{\partial c}{\partial z} = 0.$$

By introducing the dimensionless group, equation (10.a), into equations (4) and (5) and the initial and boundary conditions, the following equations (F-1) and (F-2) can be obtained

$$\frac{\partial X}{\partial \theta_i} = \frac{\partial^2 X}{\partial \lambda_i^2} - R_i(X + S_i) \qquad (F\text{-}1)$$

$$\frac{dY}{d\theta_i} + R_i(Y + S_i) = \frac{\partial X}{\partial \lambda_i}\bigg|_{\lambda_i=0}, \quad \text{for } \theta_i > 0 \qquad (F\text{-}2)$$

With new initial and boundary conditions,

(1) When $\theta_i = 0$,

$$X = 1$$

and

$$Y = 0,$$

(2) at $\lambda_i = 0$,

$$X = Y \quad \text{for } \theta_i > 0,$$

and

(3) at $\lambda_i = \alpha$,

$$\frac{\partial X}{\partial \lambda_i} = 0,$$

where

$$R_i = \frac{kL^2}{D_e \alpha^2}$$

$$S_i = \frac{c_{1i}}{c_i - c_{1i}}$$

and

$$\alpha = \frac{ALP}{V} .$$

Laplace transforms of the equations (F-1) and (F-2) are

$$\frac{d^2\overline{X}}{d\lambda_i^2} - (s + R_i)\overline{X} + 1 - \frac{R_i S_i}{s} = 0 \qquad \text{(F-3)}$$

and

$$(s + R_i)\overline{Y} + \frac{R_i S_i}{s} = \frac{d\overline{X}}{d\lambda_i}\bigg|_{\lambda_i=0} \qquad \text{(F-4)}.$$

Also, the transformed boundary conditions are written as

(i) at $\lambda_i = 0$, $\quad \overline{X} = \overline{Y} \quad$ for $\theta_i > 0$

(ii) at $\lambda_i = \alpha$, $\quad \frac{d\overline{X}}{d\lambda_i} = 0.$

The general solution for equation (F-3) can be obtained by the same method shown in Case (II); that is,

$$\bar{X} = \frac{\bar{Y} - \dfrac{s - R_1 S_1}{s(s + R_1)}}{1 + \exp(2\alpha\sqrt{s+R_1})}\left[\exp((2\alpha-\lambda_1)\sqrt{s+R_1}) + \exp(\lambda_1\sqrt{s+R_1})\right]$$

$$+ \frac{s - R_1 S_1}{s(s + R_1)} \qquad \text{(F-5)}.$$

Accordingly,

$$\bar{Y} = \frac{\exp(2\alpha\sqrt{s+R_1}) - 1}{(s + R_1)\left[\sqrt{s+R_1}(\exp(2\alpha\sqrt{s+R_1}) + 1) + (\exp(2\alpha\sqrt{s+R_1}) - 1)\right]}$$

$$- \frac{R_1 S_1}{s(s + R_1)} \qquad \text{(F-6)}.$$

Since

$$\exp(2\alpha\sqrt{s+R_1}) - 1 = 2\exp(\alpha\sqrt{s+R_1})\sinh(\alpha\sqrt{s+R_1})$$

and

$$\exp(2\alpha\sqrt{s+R_1}) + 1 = 2\exp(\alpha\sqrt{s+R_1})\cosh(\alpha\sqrt{s+R_1}),$$

equations (F-6) and (F-5) become

$$\bar{Y} = \frac{\sinh(\alpha\sqrt{s+R_1})}{(s+R_1)\left[\sqrt{s+R_1}\cosh(\alpha\sqrt{s+R_1}) + \sinh(\alpha\sqrt{s+R_1})\right]} - \frac{R_1 S_1}{s(s + R_1)} \qquad \text{(F-7)}$$

and

$$\bar{X} = \frac{1}{s+R_1} - \frac{\sqrt{s+R_1}\cosh((\alpha-\lambda_1)\sqrt{s+R_1})}{(s+R_1)\left[\sqrt{s+R_1}\cosh(\alpha\sqrt{s+R_1}) + \sinh(\alpha\sqrt{s+R_1})\right]}$$

$$- \frac{R_1 S_1}{s(s+R_1)} \qquad \text{(F-8)}.$$

By the same procedure as that in Appendix (C), the inverse Laplace transforms of $\bar{Y}(s)$ and $\bar{X}(s,\lambda_i)$, $Y(\theta_i)$ and $X(\theta_i, \lambda_i)$, can be obtained as follows:

$$Y(\theta_i) = \frac{\alpha}{1+\alpha} \exp(-R_i\theta_i) - \sum_{n=1}^{\infty} \frac{2}{1+\alpha+\alpha\delta_n^2} \exp(-(\delta_n^2 + R_i)\theta_i)$$

$$- S_i(1 - \exp(-R_i\theta_i)) \qquad \text{(F-9)}$$

and

$$X(\theta_i,\lambda_i) = \frac{\alpha}{1+\alpha} \exp(-R_i\theta_i)$$

$$- \sum_{n=1}^{\infty} \frac{2 \cos[\delta_n(\alpha-\lambda_i)]}{(1+\alpha+\alpha\delta_n^2) \cos \alpha\delta_n} \exp(-(\delta_n^2+R_i)\theta_i)$$

$$- S_i(1 - \exp(-R_i\theta_i)) \qquad \text{(F-10)}$$

where δ_n satisfies

$$\cot(\alpha\delta) + 1 = 0 \qquad \text{(F-11)}.$$

APPENDIX. G.

Fig. G-1. Computer logic chart to minimize $E = E(x)$, $c \leq x \leq d$ using Golden Section search.

Table. G-1. Computer program for Golden Section search.

Table. G-2. Program symbols and explanation.

Fig. G-2. Determination of K and L_o by two dimensional search technique (Box Method).

Table. G-3. Computational values of K, L_o, and E for Run (8).

Table. G-4. Experimental data for Run (5).

Table. G-5. Experimental data for Run (6).

Table. G-6. Experimental data for Run (8).

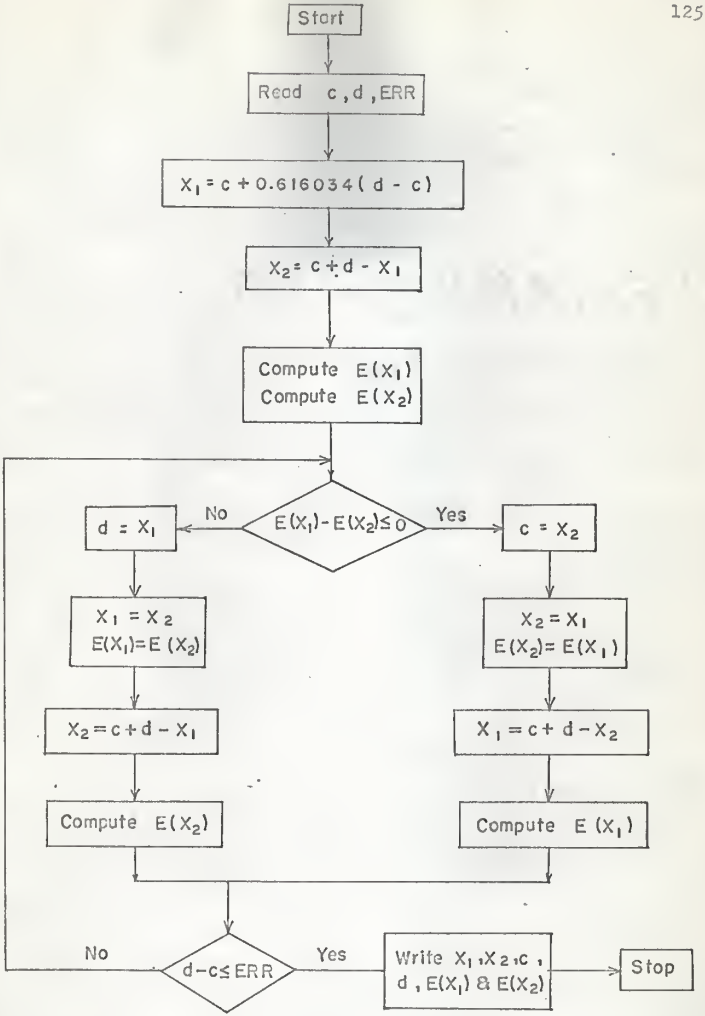

Fig. G-1. Computer logic chart to minimize $E = E(X)$, $c \leq x \leq d$ using Golden Section Search.

Table. G-1. Computer program for Golden Section search.

```
$JOB            SRC,RUN=CHECK,TIME=01,PAGES=20,LINES=47
C
C
C     ONE DIMENSIONAL GOLDEN SECTION SEARCH TECHNIQUE
C
C
      DIMENSION X(2),W(2)
  101 FORMAT(5F12.6)
  106 FORMAT(6H W(K)=E14.7,6H X(K)=E14.7,3H C=E14.7,3H D=E14.7)
  107 FORMAT(//11H **********,23X,11H **********,23X,11H **********//)
  108 FORMAT(22H THE WORK IS COMPLETED)
      READ(1,101) C,D,ERR
      WRITE(3,101) C,D,ERR
      X(1)=C+0.618034*(D-C)
      X(2)=C+D-X(1)
      K=1
C
C     THE USER MUST PROVIDE THE OBJECTIVE FUNCTION FOR OBTAINING
C     THE REQUIRED FUNCTION VALUE AT EACH  POINT BETWEEN THIS
C     COMMENT STATEMENT AND THE FOLLOWING STATEMENT IN WHICH
C     E MEANS THE REQUIRED FUNCTION VALUE.
C
C     IN THIS CASE THE OBJECTIVE FUNCTION FOR DETERMINING DE IS
C     USED AS AN ILLUSTRATION.
C
C
      DIMENSION B(21),T(50),CL(50),DE(2),P2(2,21),P3(2,21),P4(2,21),YC(2
     1,50),YE(50),Y(2,50)
  100 FORMAT(6F12.5)
  102 FORMAT(5F14.6)
  103 FORMAT(7F10.4)
  105 FORMAT(5F14.9)
      READ(1,100) A,P,FL,VV
      WRITE(3,100) A,P,FL,VV
      READ(1,102) (B(J),J=1,20)
      WRITE(3,102) (B(J),J=1,20)
      READ(1,103) (T(I),I=1,13)
      WRITE(3,103) (T(I),I=1,13)
      READ(1,105) (YE(I),I=2,13)
      WRITE(3,105) (YE(I),I=2,13)
C
C     WHEN THIS TECHNIQUE IS USED FOR THE PURPOSE OF DETERMINING
C     DE, X(K)=DE(K).
C
   10 DO 50 K=1,2
      E=0.
      DE(K)=X(K)
```

Table. G-1. Computer program for Golden Section search(cont'd).

```
      DO 45 I=1,13
      S=0.
      P1=1./(1.+VV/(A*P*FL))*100000.*30000.
      DO 40 J=1,20
      P2(K,J)=2.*30000.*EXP(-DE(K)*B(J)*B(J)*T(I)/(FL*FL))*100000.
      P3(K,J)=(1.+A*FL*P/VV+VV*B(J)*B(J)/(A*P*FL))
      P4(K,J)=P2(K,J)/P3(K,J)
      S=S+P4(K,J)
   40 CONTINUE
      YC(K,I)=(P1-S)/(30000.*100000.)
      Y(K,I)=YC(K,I)-YC(K,1)
      IF(I.EQ.1) GO TO 45
      E=E+(Y(K,I)-YE(I))*(Y(K,I)-YE(I))
   45 CONTINUE
      W(K)=E
      X(K)=DE(K)
C
      WRITE(3,106) W(K),X(K),C,D
      GO TO(50,24,25),M
   50 CONTINUE
   21 IF(W(1)-W(2))22,22,23
   22 C=X(2)
      X(2)=X(1)
      W(2)=W(1)
      X(1)=C+D-X(2)
      M=2
      GO TO 10
   24 IF(ABS(D-C)-ERR)26,26,21
   23 D=X(1)
      G=X(2)
      H=W(2)
      X(1)=D+C-G
      M=3
      GO TO 10
   25 X(2)=X(1)
      W(2)=W(1)
      X(1)=G
      W(1)=H
      GO TO 24
   26 WRITE(3,107)
      WRITE(3,106) W(K),X(K),C,D
      WRITE(3,107)
      WRITE(3,105) (YC(K,I),I=1,13)
      WRITE(3,107)
      WRITE(3,108)
      STOP
      END
```

Table. G-2. PROGRAM SYMBOLS AND EXPLANATION

Program Symbols	Explanation	Mathematical Symbols
A	cross-sectional area, cm^2	A
B(J)	jth eigenvalues	β_j
C	lower limit of the independent variable	
CL(I)	concentration of the ith sample solution, g-moles/liter or mg/liter	c_l
D	upper limit of the independent variable	
DE	effective pseudo-molecular diffusivity, cm^2/sec	D_{pe}
ERR	prescribed accuracy of the function value for stopping the computation	
FL	corrected thickness of the packed bed, cm	L_c
P	porosity of the packed bed	P
T(I)	time at which ith sample was taken, sec	t
VV	corrected upper reservoir's volume, cm^3	V_c
W(K)	kth value of the objective function	E
X(K)	kth value of the independent variable	D_{pe} or L_o^{pe}
YC(K,I)	dimensionless theoretical concentration at T(I) when X(K) is used	Y_c
YE(I)	dimensionless experimental concentration of CL(I)	Y_e

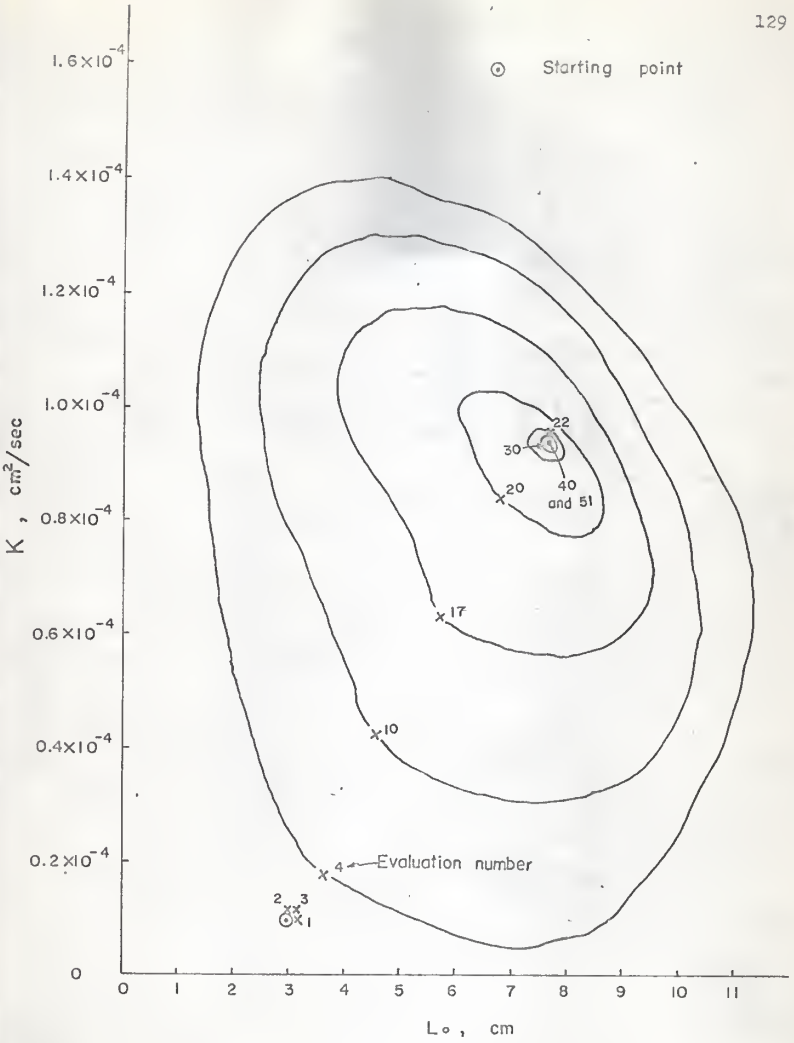

Fig. G-2 . Determenation of K & L_o by two dimensional search technique (Box method).

Table. G-3. Computational values of K, L_o and E for Run (8)

number of evaluation	K (cm^2/sec)	L_o (cm)	E
1	1.000×10^{-5}	0.3150	3.0237×10^{-2}
2	1.139×10^{-5}	0.3000	2.9126×10^{-2}
3	1.139×10^{-5}	0.3150	2.8695×10^{-2}
4	1.791×10^{-5}	0.3651	2.1636×10^{-2}
10	4.250×10^{-5}	0.4554	8.4640×10^{-3}
17	6.301×10^{-5}	0.5737	2.9012×10^{-3}
20	8.403×10^{-5}	0.6807	5.6018×10^{-4}
22	9.575×10^{-5}	0.7694	2.5552×10^{-4}
30	9.292×10^{-5}	0.7564	2.5387×10^{-4}
40	9.428×10^{-5}	0.7657	2.5085×10^{-4}
50	9.369×10^{-5}	0.7622	2.5094×10^{-4}
51	9.428×10^{-5}	0.7657	2.5085×10^{-4}

Table. G-4. Experimental data for Run (5)

L_o = 0.6958 cm
c_{lci} = 0.29185 moles/liter

time (hrs)	position (H=high, L=low)	refractive index	wt % conc.	temp. (°C)	temp. correction (wt %)	wt % by refracto-meter	real wt %	molar conc. (moles/l)	average molar conc. (moles/l)	corrected dimensionless conc., Y_c
3	H	1.34685	9.40	25.20	0.374	9.774	9.66	0.2926	0.2926	0.001134
		1.34685	9.40	25.20	0.374	9.774	9.66	0.2926		
	L	1.34685	9.40	25.20	0.374	9.774	9.66	0.2926		
		1.34683	9.40	25.20	0.374	9.774	9.66	0.2926		
11 5/6	H	1.34685	9.40	25.00	0.360	9.760	9.65	0.2923	0.29245	0.000906
		1.34695	9.42	25.00	0.360	9.780	9.67	0.2929		
	L	1.34690	9.40	25.00	0.360	9.760	9.65	0.2923		
		1.34690	9.40	25.00	0.360	9.760	9.65	0.2923		
14	H	1.34680	9.38	25.20	0.374	9.754	9.64	0.2919	0.29243	0.000876
		1.34685	9.39	25.20	0.374	9.764	9.65	0.2923		
	L	1.34687	9.40	25.20	0.374	9.774	9.66	0.2926		
		1.34690	9.41	25.20	0.374	9.784	9.67	0.2929		
16	H	1.34700	9.48	24.35	0.308	9.788	9.68	0.2932	0.2939	0.003112
		1.34715	9.55	24.40	0.312	9.862	9.75	0.2954		
	L	1.34700	9.50	24.30	0.304	9.804	9.69	0.2935		
		1.34700	9.50	24.30	0.304	9.804	9.69	0.2935		
19	H	1.34712	9.58	24.45	0.316	9.896	9.78	0.2963	0.2962	0.006611
		1.34715	9.59	24.45	0.316	9.906	9.79	0.2967		
	L	1.34725	9.60	24.45	0.316	9.916	9.80	0.29698		
		1.34710	9.53	24.45	0.316	9.846	9.73	0.2948		

Table. G-4. Experimental data for Run (5) (continued)

L_o = 0.6958 cm
c_{lci} = 0.29185 moles/liter

Time (hrs)	position (H;high) (L;low)	refractive index	wt % conc.	temp. (°C)	temp. correction (wt %)	wt % by refracto-meter	real wt %	molar conc. (moles/l)	average molar conc. (moles/l)	corrected dimensionless conc., Y_c
23	H	1.34725	9.65	24.50	0.320	9.970	9.86	0.2989	0.29636	0.006854
		1.34725	9.63	24.50	0.320	9.950	9.84	0.29824		
	L	1.34700	9.50	24.50	0.320	9.820	9.71	0.29415		
		1.34710	9.50	24.50	0.320	9.820	9.71	0.29415		
26	H	1.34725	9.63	24.40	0.312	9.942	9.83	0.2979	0.29776	0.008084
		1.34725	9.63	24.40	0.312	9.942	9.83	0.2979		
	L	1.34720	9.60	24.40	0.312	9.912	9.80	0.29698		
		1.34725	9.64	24.40	0.312	9.952	9.84	0.29824		
37½	H	1.34754	9.84	23.20	0.224	10.064	9.95	0.3017	0.30171	0.014993
		1.34755	9.85	23.20	0.224	10.074	9.96	0.3020		
	L	1.34750	9.31	23.20	0.224	10.034	9.92	0.3008		
		1.34757	9.86	23.20	0.224	10.084	9.97	0.30234		
39½	H	1.34750	9.82	23.45	0.2415	10.0615	9.95	0.3017	0.30245	0.016119
		1.34760	9.87	23.50	0.245	10.115	10.00	0.3033		
	L	1.34750	9.81	23.35	0.2345	10.0445	9.93	0.3012		
		1.34765	9.90	23.35	0.2345	10.1345	10.01	0.3036		
44	H	1.34760	9.90	23.25	0.2275	10.1275	10.01	0.3035	0.3022	0.015738
		1.34760	9.88	23.25	0.2275	10.1075	9.99	0.3030		
	L	1.34752	9.84	23.25	0.2275	10.0675	9.95	0.3017		
		1.34750	9.80	23.25	0.2275	10.0275	9.91	0.3005		

Table. G-5. Experimental data for Run (6)

L_o = 3.4874 cm
c_{lci} = 0.34400 moles/liter

time (hrs)	position H=high L=low	refractive index	wt % conc.	temp. (°C)	temp. correction (wt %)	wt % by refracto-meter	real wt %	molar conc. (moles/l)	average molar conc. (moles/l)	corrected dimensionless conc., $\bar{c}_c$
7	H	1.3500	11.45	20	0.00	11.45	11.32	0.3451	0.34543	0.004164
		1.34955	11.17	24	0.28	11.45	11.32	0.3451		
	L	1.34955	11.18	24	0.28	11.46	11.33	0.3454		
		1.34965	11.20	24	0.28	11.48	11.35	0.3461		
9	H	1.3498	11.30	22	0.14	11.44	11.31	0.3448	0.34538	0.004018
		1.3497	11.22	24	0.28	11.50	11.37	0.3467		
	L	1.34957	11.20	24	0.28	11.48	11.35	0.3461		
		1.34950	11.13	24	0.28	11.41	11.28	0.3439		
11 1/6	H	1.34975	11.25	23	0.21	11.46	11.33	0.3454	0.34575	0.005095
		1.34995	11.40	23	0.21	11.61	11.48	0.3502		
	L	1.34955	11.17	24	0.28	11.45	11.32	0.3451		
		1.34950	11.03	24	0.28	11.36	11.23	0.3423		
12 1/6	H	1.34955	11.17	24	0.28	11.45	11.32	0.3451	0.34430	0.00873
		1.34960	11.20	24	0.28	11.48	11.35	0.3461		
	L	1.34945	11.05	24	0.28	11.33	11.20	0.3413		
		1.34955	11.15	24	0.28	11.43	11.30	0.3447		
21	H	1.34980	11.33	21.6	0.11	11.44	11.31	0.3449	0.34570	0.004950
		1.3500	11.40	21.6	0.11	11.51	11.38	0.3471		
	L	1.34970	11.22	23.4	0.24	11.46	11.33	0.3454		
		1.34970	11.22	23.4	0.24	11.46	11.33	0.3454		

Table. G-5. Experimental data for Run (6)(continued)

L_o = 3.4874 cm
c_{lci} = 0.34400 moles/liter

time (hrs)	position H:high L:low	refractive index	wt % conc.	temp. (°C)	temp. correction (wt %)	wt % by refracto-meter	real wt %	molar conc. (moles/l)	average molar conc. (moles/l)	corrected dimensionless conc., Y_c
23	H	1.34975	11.24	23.5	0.25	11.49	11.36	0.3464	0.34713	0.009114
		1.34980	11.30	23.5	0.25	11.55	11.42	0.3483		
	L	1.34980	11.30	22.5	0.18	11.48	11.35	0.3461		
		1.34990	11.35	22.5	0.18	11.53	11.40	0.3477		
25	H	1.34975	11.25	23.3	0.23	11.48	11.35	0.3461	0.34675	0.003008
		1.34979	11.30	23.3	0.23	11.53	11.40	0.3477		
	L	1.34975	11.25	23.3	0.23	11.48	11.35	0.3461		
		1.34977	11.28	23.3	0.23	11.51	11.38	0.3471		
34	H	1.35010	11.55	20.0	0.0	11.55	11.42	0.3483	0.34833	0.012609
		1.35000	11.43	20.0	0.0	11.43	11.30	0.3445		
	L	1.35025	11.60	20.0	0.0	11.60	11.47	0.3499		
		1.35035	11.62	20.0	0.0	11.62	11.49	0.3506		
35	H	1.35030	11.62	20.0	0.0	11.62	11.49	0.3506	0.3478	0.011065
		1.35005	11.42	20.0	0.0	11.42	11.29	0.3443		
	L	1.35023	11.59	20.0	0.0	11.59	11.46	0.3496		
		1.35010	11.50	20.0	0.0	11.50	11.37	0.3467		
	H									
	L									

Table. G-6. Experimental data for Run (8)

$K = 9.428 \times 10^{-5}$ cm²/sec

$L_o = 0.7657$ cm

$c_{1ci} = 0.38635$ moles/liter

Time (hrs.)	position (U=high, L=low)	refractive index	wt % conc.	temp. (°C)	temp. correction (wt %)	wt % by refracto-meter	real wt %	molar conc. (moles/l)	average molar conc. (moles/l)	corrected dimensionless conc., Y_c
2		1.35195	12.64	24.00	0.285	12.925	12.782	0.3920	0.3947	0.017583
		1.35220	12.81	24.00	0.285	13.095	12.950	0.3974		
3		1.35240	12.98	22.00	0.140	13.120	12.975	0.3982	0.3962	0.020735
		1.35230	12.85	22.00	0.140	12.990	12.846	0.3941		
4		1.35200	12.68	24.10	0.293	12.973	12.829	0.3935	0.3958	0.019395
		1.35222	12.82	24.10	0.293	13.113	12.968	0.3980		
5		1.35240	12.92	24.25	0.305	13.225	13.079	0.4016	0.3998	0.028300
		1.35245	12.98	24.25	0.305	13.113	12.968	0.3980		
6		1.35250	13.00	23.50	0.250	13.250	13.104	0.4024	0.4005	0.029771
		1.35250	13.00	21.90	0.135	13.135	12.990	0.3986		
7½		1.35230	12.85	24.00	0.285	13.135	12.990	0.3986	0.4008	0.030402
		1.35242	12.98	24.00	0.285	13.265	13.119	0.4029		
9		1.35275	13.18	21.50	0.105	13.285	13.138	0.4035	0.4027	0.034394
		1.35265	13.13	21.50	0.105	13.235	13.089	0.4019		
10		1.35260	13.10	22.00	0.140	13.240	13.094	0.4021	0.4037	0.036496
		1.35280	13.20	22.00	0.140	13.340	13.193	0.4053		
11		1.35282	13.21	21.50	0.105	13.315	13.168	0.4045	0.4040	0.037126
		1.35275	13.18	21.50	0.105	13.285	13.138	0.4035		
12½		1.35285	13.22	22.00	0.140	13.36	13.213	0.4059	0.4075	0.044491
		1.35298	13.32	22.00	0.140	13.46	13.312	0.4091		

Table. G-6. Experimental data for Run (8)(continued)

$K = 9.428 \times 10^{-5}$ cm²/sec
$L_o = 0.7657$ cm
$c_{1c1} = 0.38635$ moles/liter

Time (hrs)	position (highest to lowest)	refractive index	wt % conc.	temp. (°C)	temp. correction (wt %)	wt % by refracto-meter	real wt %	molar conc. (moles/l)	average molar conc. (moles/l)	corrected dimensionless conc., Y_c
14		1.35283	13.22	22.00	0.14	13.36	13.213	0.4059	0.4077	0.044902
		1.35299	13.33	22.00	0.14	13.47	13.321	0.4094		
15½		1.35270	13.28	22.00	0.14	13.42	13.272	0.4078	0.4073	0.044061
		1.35290	13.25	22.00	0.14	13.39	13.242	0.4068		
17		1.35295	13.28	22.00	0.14	13.42	13.272	0.4078	0.4078	0.045112
		1.35295	13.28	22.00	0.14	13.42	13.272	0.4078		
20		1.35330	13.55	21.00	0.07	13.62	13.470	0.4142	0.4143	0.058771
		1.35335	13.58	21.00	0.07	13.65	13.500	0.4152		
		1.35330	13.53	21.00	0.07	13.60	13.450	0.4136		
24		1.35335	13.61	22.00	0.14	13.75	13.599	0.4184	0.4168	0.064025
		1.35300	13.51	22.00	0.14	13.65	13.500	0.4152		
27		1.35315	13.44	23.55	0.25	13.69	13.539	0.4165	0.4185	0.067597
		1.35325	13.51	23.55	0.25	13.75	13.599	0.4184		
		1.35334	13.57	23.55	0.25	13.82	13.668	0.4207		
29		1.35350	13.60	23.00	0.21	13.81	13.658	0.4203	0.4215	0.073901
		1.35355	13.61	23.00	0.21	13.82	13.668	0.4207		
		1.35350	13.60	23.00	0.21	13.81	13.658	0.4203		

[illegible]

by

SO KWANG CHOI

B. S., Seoul National University, 1966

AN ABSTRACT OF A MASTER'S THESIS

submitted in partial fulfillment of the

requirements for the degree

MASTER OF SCIENCE

Department of Chemical Engineering

KANSAS STATE UNIVERSITY
Manhattan, Kansas

1969

ABSTRACT

It has been known that runoff from cattle feedlots is a significant source of water pollution in the Midwest, where commercial cattle feeding has grown rapidly. In the runoff stream, the chemical oxygen demand (COD) is one measure of the concentration of the organic components which contaminate water.

To determine the transport rate of manure through a porous stratum saturated by water under the simulated condition of the feedlot, a mathematical model of the system consisting of the soil-manure packed bed saturated by water and the well mixed solution on the bed was established. For this mathematical model, the system equations and the corresponding initial and boundary conditions were derived for several cases. For those cases, the analytical expressions for the concentrations within the packed bed and in the upper solution were obtained as the function of time and distance from the interface of the two layers and as the function of time respectively.

To apply the experimental set-up of the mathematical model for the purpose of determining the transport rate of manure as measured by its COD through the porous bed, the experimental set-up was tested and calibrated by the experiments with an aqueous sucrose solution of known diffusivity. It was shown that a single correction factor in terms of the depth correction factor satisfactory corrected the effects due to the initial disturbance and the continuous convective motion of the fluid.

The experimental system which had been characterized as

[illegible] the transport rate of manure as measured by its COD through the porous bed. Since the diffusivity (pseudo-molecular diffusivity) of manure is necessary, it was obtained by forcing the experimental data to fit the mathematical model. The Golden Section search technique was used for this purpose. The effective diffusivity through the porous bed saturated by water (effective pseudo-diffusivity) of manure as measured by its COD was found to be approximately 5.02×10^{-6} cm^2/sec at the temperature of 25±2 °C. This corresponds to a molecular (pseudo-molecular) diffusivity of 7.10×10^{-6} cm^2/sec.

Information generated in this study is pertinent to water pollution caused by feedlot runoff. Since the effective diffusivity (effective pseudo-diffusivity) of manure through a porous stratum is small, it can be said that organic matter which diffuses from the earth beneath the feedlot to the surface of the feedlot does not probably contribute seriously to the pollution due to the feedlot runoff. It may be concluded that as far as COD is concerned, manure suspension in the runoff water contributes mainly to water pollution. This work can also be applied to study the effect of diffusivity of a substance in the process of fluid flowing through a porous bed such as soil.